University of Alberta

NODE SWITCHING RATE IN COOPERATIVE COMMUNICATIONS

by

Chuzhe Xiao

A thesis submitted to the Faculty of Graduate Studies and Research in partial fulfillment of the requirements for the degree of

Master of Science

in

Communications

Department of Electrical and Computer Engineering

Fall 2012
Edmonton, Alberta

This work is dedicated to my parents.

Abstract

In opportunistic relaying systems, only the relay with best channel condition among K relays is selected to take part in cooperation. This setup efficiently achieves diversity gain. However, the high switching rate of such systems may be undesirable due to practical implementation issues, for example, the corruption of the data signal by receiver switching transients, or channel estimation and synchronization failures due to excessive switching, as well as network control switching overheads which increase with increased switching. Recently, switch-and-examine relaying whose main advantage is its low switching rate, was proposed as a low complexity suboptimal alternative to opportunistic relaying. Meanwhile, comparisons of the switching rates of opportunistic and switch-and-examine schemes have been undertaken only for the case of Rayleigh fading. In this thesis, the switching rates of opportunistic relaying and switch-and-examine relaying systems with two or more relays operating under Rician and Nakagami-*m* fading are obtained in closed-form or single integral expressions. Results for independent and identically distributed fading links are obtained for the case of multiple relays and additionally for independent but not identically distributed fading links for the two relays case. The closed-form solutions explicitly depend on the Doppler frequency of the fading.

Acknowledgements

First and foremost I would like to offer my sincerest gratitude to my supervisor, Dr. Norman C. Beaulieu for his continuous support, patience and encouragement during my graduate studies. This thesis would not have been possible without his vast knowledge, experience and constructive suggestions.

I would also like to express my appreciation to the members of my defense committee, Dr. Hai Jiang and Dr. Ioanis Nikolaidis for reviewing my thesis.

My special thanks go to Kasun Hemachandra, Sijing Jiang, Gayan Amarasuriya, Payam Dehghani Rahimzadeh and Xin Wang and many more for their generous support and help with my research. I would also like to thank all the members of the *i*CORE Wireless Communication Laboratory for creating a professional and supporting environment.

Finally I am extremely grateful to my family for their unconditional love and support. It is their encouragement that get me through the most difficult time and make everything I accomplished possible.

Contents

List of Figures

List of Symbols

List of Abbreviations

Chapter 1

Introduction

The first decade of the 21st century witnessed an unprecedented rapid growth in wireless communication technologies. One of the main technological advancements that enables such dramatic growth is the deployment of multiple-input multiple-output (MIMO) technology. In MIMO systems, both the transmitter and the receiver employ multiple antennas in order to obtain higher data rates and/or to alleviate channel impairments (such as noise, fading and shadowing effects). However, while MIMO technology has been tremendously successful, it may not be an ideal solution for many practical wireless networks due to cost, complexity and hardware constraints. One of the most promising alternatives to MIMO technology is cooperative relaying.

1.1 Cooperative Relaying

Cooperative relaying has received great attention in recent years as an alternative and improvement to MIMO technology because it can also enhance the reliability of data transmission, provide broader and cheaper coverage and mitigate severe shadowing and fading effects [1]. In conventional communication systems, the source (transmitter) and the destination (receiver) communicate directly without any outside help. However, in cooperative relaying systems, the source and the destination communicate with each other with the help of one or more relays.

A single-hop relaying scheme is illustrated in Fig. 1.1. The protocol in [1] divided data transmission into two phases. In the first phase, the source transmits

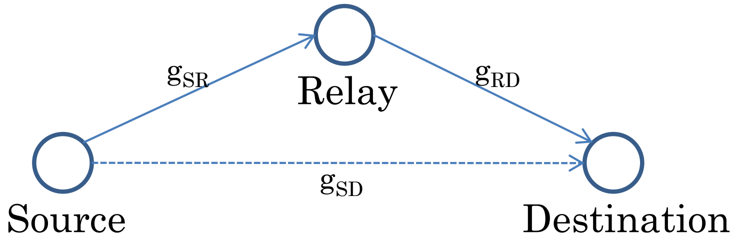

Figure 1.1. A cooperative relaying system with one relay.

some data to the destination as in conventional communication systems. Due to the broadcast nature of wireless communication, the relay also receives a copy of the data. In the second phase, the relay processes the received data then forwards it to the destination. The destination will then decode the data using the two replicas it received (one from the source and the other from the relay). Since the destination node utilizes signals from both source and destination, diversity can be achieved. Evidently, how the relay processes the data will have a major impact on the system performance metrics, especially bit error rate (BER) and outage probability (OP). In the literature, there are currently two popular methods, amplify-and-forward (AF) and decode-and-forward (DF). In AF, the relay will simply amplify the received signal (by a fixed factor or by a variable factor to normalized the energy) and then transmit it. In DF, the relay will decode the received signal and then re-encode and transmit it.

1.2 Opportunistic Relaying and Switch-and-Examine Relaying

In [1], only one relay is available for cooperation, while in practice multiple relays may be employed to further improve performance. One way to exploit the diversity gain in such systems is to use distributed space-time coding at the relays [2]. However, the code design for such system is difficult because the number of nodes participating in cooperation may not been known *a priori*. The authors in [3] proposed opportunistic relaying (OR) as a scheme for multiple relay systems, in which only the relay with the best channel condition participates in cooperation actively, while all the other relays cooperate ”passively” by not transmitting information.

OR has been shown to achieve full diversity with relatively low complexity [3], [4]. Despite the benefits offered by OR, one of the issues that must be addressed in practice is its high switching rate, i.e. the number of times per second the system has to switch from one relay node to another, especially when the number of relays is large or the channel conditions change frequently. In conventional receiver diversity combining systems, switched diversity has been implemented as a low complexity suboptimal alternative to selection diversity to reduce the antenna switching rate [5]. Applying this idea to relaying systems, the authors in [6] proposed and studied switch-and-stay relaying systems with two relays. In switch-and-stay relaying, the systems dwells on one relay as long as its channel condition is better than a predetermined threshold. Once its channel condition crosses below the threshold, the system switches to the other relay. An important insight uncovered in [6] is that switch-and-stay relaying achieves the same diversity order as opportunistic relaying while reducing the switching rate. Note that switch-and-stay relaying refers to systems with only two relays. In this thesis, we intend to investigate systems with more than two relays, thus we use the term “switch-and-examine relaying” to refer to such systems.

1.3 Thesis Motivation and Contributions

This thesis is devoted to investigating the switching rate in opportunistic relaying and switch-and-examine relaying.

It is desirable to keep the switching rates in relaying networks as low as possible for several reasons, both from the node perspective and from the network perspective. The switching rates are critically important at the node receiver for two reasons. First, in order to coherently decode the received message, the relay node and the destination require accurate channel estimation which is impossible unless the system dwells on a specific relay node for a long enough time [7]. Excessive switching will undermine the accuracy of channel estimation, which in turn will degrade the system performance. Secondly, relay nodes are implemented by ordinary electrical circuits which have certain transient responses. Whenever the system switches to a new relay, it is equivalent to applying a step function input to the new relay node receiver. The triggered receiver transient response will corrupt any signal received and cause an ”internal outage” [8], [9]. Note that highpass responses in any receiver elements (RF amplifiers and filters, IF amplifiers and filters, demodulator circuits) may cause transients lasting thousands of symbol durations [10]. In order to evaluate the impacts of such internal outage, one would have to consider a particular receiver. Then one needs to obtain the impulse response of the underlying circuits and the dwell time of a specific relay (how long the system communicates with a specific relay before switching). We focus on the more fundamental issue of switching rate in this thesis and do not address receiver-specific questions. Future research could investigate this issue in more detail. From the network perspective, excessive switching may cause network synchronization failures or delays due to the distributed nature of cooperative relaying systems [11]. Every switch from one relay to another requires a new time synchronization in that the time delay associated with one relay can be dramatically different from that associated with another relay.

While the switching rate is of paramount importance to practical implementation of opportunistic relaying and switch-and-examine relaying systems, current literature does not address it adequately. The majority of the literature concerning multiple relay systems has investigated the bit error rate and outage probability of such systems without considering the detrimental effect of switching rate. To fully understand the impact of switching rate in cooperative communication systems, one has to first investigate what is the value of switching rate in various scenarios.

The switching rates for these two systems in Rayleigh fading channels have been investigated in [11]. However, Rayleigh fading may be an inadequate model for practical channels, for example channels with a line-of-sight (LOS) component or channels suffering from more severe fading or less severe fading than Rayleigh fading. Therefore, it is essential to investigate switching rates in more flexible fading models, such as Rician fading and Nakagami-m fading. To the best of the author's knowledge, no such results are available in the literature. In this thesis, the switching rates for dual-branch and multi-branch[1] opportunistic relaying and switch-and-examine relaying undergoing both Rician and Nakagami-*m* fading are derived. Note that the switching rate discussed here is driven by and explicitly depends on the maximum Doppler shift. This is different from what is termed the switching rate in [12], where the maximum Doppler shift is effectively zero.

1.4 Thesis Outline

The remainder of this thesis is organized as follow. Chapter 2 introduces the system models under consideration. Fading channels and the transmission protocols used by opportunistic relaying and switch-and-examine relaying are discussed. In Chapter 3, we derive the switching rate for both dual-branch and multi-branch systems analytically. For Rician fading, the results are presented in single-integral form, while for Nakagami-*m* fading, closed-form results are available in addition to single-integral form. Chapter 4 gives the switching rates of the switch-and-examine relaying. The results are presented in closed-form. Then, Chapter 5 gives numerical examples to illustrate the theoretical results. Numerical examples demonstrate how different parameters affect the switching rate. Finally, Chapter 6 concludes the thesis and discusses possible future research in this field.

[1] In the literature, dual-branch and multi-branch systems are sometimes referred to as two-relay and multi-relay systems, respectively. Both nomenclatures are used in this thesis.

Chapter 2

System Models

In this chapter, the models used in this thesis are presented. Specifically, fading channels are discussed and the models used by opportunistic relaying and switch-and-examine relaying are presented.

We consider a dual-hop multi-branch cooperative relaying system in which a source terminal, S, communicates with a destination terminal, D, with the help of L relaying terminals denoted by T_i, $i \in 1, ..., L$. The system model is illustrated in Fig. 2.1.

2.1 Fading Channels

In wireless communication systems, one major characteristic is that there are many signal paths from the transmitter to the receiver due to refractions, reflections and scattering of the transmitted signal in the local environment. Therefore the received signal will appear as a pulse train and different replicas of the received signal will add constructively and destructively. This process is further complicated by the relative motion between transmitter and receiver. The end result is random fluctuations of amplitude, phase and power of the received signal in time, frequency and space. This communication channel is referred to as a multipath fading channel [13] [14].

Two important parameters in multipath fading are coherence bandwidth and coherence time. Coherence bandwidth is the frequency range over which the fading process is considered highly correlated. The coherence bandwidth can be defined as the inverse of the time delay spread, which is the time difference between the first

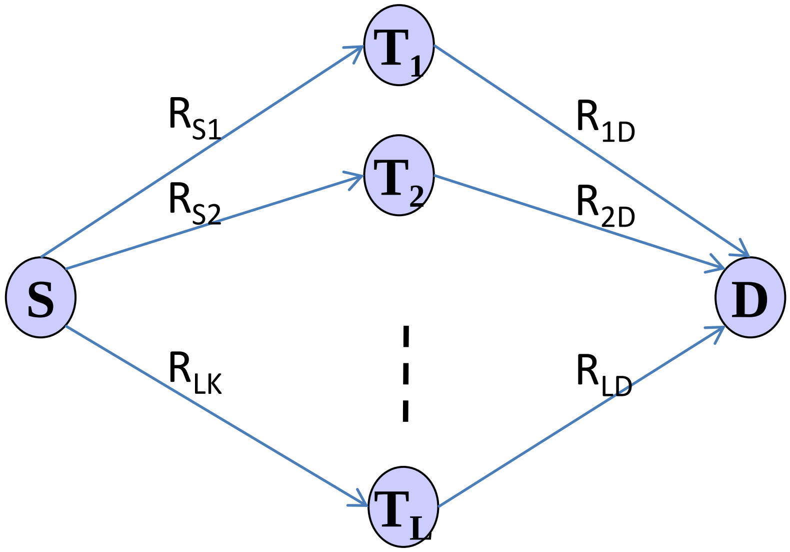

Figure 2.1. A cooperative relaying system with L multiple relays.

replica of received signal and the last replica of received signal. If the bandwidth of transmitted signal is much smaller than the coherence bandwidth, we can consider the fading process to be flat in the frequency domain. Such a fading process is called flat fading. If the bandwidth of transmitted signal is much larger than the coherence bandwidth, the fading process has significant variation in the frequency domain, and we call such a fading process frequency selective fading.

On the other hand, coherence time is the time period over which the fading process is considered highly correlated. The coherence time of a fading channel is usually defined as the inverse of the Doppler spread. The relative motion between transmitter and receiver introduces frequency shift, called Doppler shift, in the received signal along each signal path, which is known as the Doppler effect. Signals along different paths can have different Doppler shifts, and the difference between the maximum Doppler shift and the minimum Doppler shift is defined as the Doppler spread. If the symbol duration is smaller than the coherence time, we can consider the amplitude and phase of the fading process to be constant over the period of use. Such a fading process is called slow fading. If the symbol duration is greater than the coherence time, the amplitude and phase of the fading process varies considerably over the period of use.

In this thesis, we assume the fading process to be both flat and fast. In these cases, it is common to use statistical models to capture the random nature of the received signal amplitude. Note that coherent detection assumes that the receiver fully compensates for the received signal phase; thus, its distribution is not relevant in this thesis. Three most widely used models for received signal amplitude include Rayleigh fading, Rician fading and Nakagami-*m* fading. Rayleigh fading is often used to model the channel amplitude in a wireless system with no direct LOS path between the transmitter and the receiver and only scattering components. Meanwhile, Rician fading is often used to model systems where a LOS component is present in addition to scattering components. Unfortunately, some experimental data does not fit well into either of these distributions. Thus Nakagami-*m* fading has been proposed to fit empirical measurements. Note that the Rayleigh model is a special case of both Rician and Nakagami-*m* fading.

We assume that the channel between terminals A and B (A or B can be the source, the destination or the relay T_i) undergoes fast fading with channel gain R_{AB} and maximum Doppler frequency f_{AB}; the fadings on different channels are assumed to be independent but not identically distributed (i.n.i.d.). Let R_{Si} and f_{Si} denote the channel amplitude and the maximum Doppler frequency between the source and relaying terminal T_i, respectively. We assume that R_{AB} experiences Rician or Nakagami-*m* fading. For Rician fading, the probability density function (PDF), $f_{R_{AB}}(r)$, and cumulative distribution function (CDF), $F_{R_{AB}}(r)$, are given by [15]

$$f_{R_{AB}}(r) = \frac{r}{\sigma_{AB}^2} \exp\left(-\frac{r^2}{2\sigma_{AB}^2} - K_{AB}\right) I_0\left(\sqrt{2K_{AB}}\frac{r}{\sigma_{AB}}\right) \tag{2.1}$$

$$F_{R_{AB}}(r) = 1 - Q_1\left(\sqrt{2K_{AB}}, \frac{r}{\sigma_{AB}}\right) \tag{2.2}$$

where $I_0(x)$ is the modified Bessel function of the first kind of order zero as defined in [16, eq. (8.406.1)] and $Q_1(a,b)$ is the Marcum Q function as defined in [17, eq. (2.20)]. Also, K_{AB} and $2\sigma_{AB}^2$ are the Rice factor and average power in the scatter component, respectively. Note that K_{AB} is a indicator of the severity of the fading and can be any value between 0 to ∞. A small K_{AB} implies severe fading, while a large K_{AB} indicates mild fading. When $K_{AB} = 0$, Rician fading reduces to Rayleigh fading and when $K_{AB} = \infty$, we have no fading (a channel with only LOS component).

Similarly, for Nakagami-*m* fading, the PDF and CDF are given by [15]

$$f_{R_{AB}}(r) = \frac{2r^{2m_{AB}-1}}{\Gamma(m_{AB})}\left(\frac{m_{AB}}{\Omega_{AB}}\right)^{m_{AB}} \exp\left(-\frac{m_{AB}r^2}{\Omega_{AB}}\right) \tag{2.3}$$

$$F_{R_{AB}}(r) = \frac{\gamma\left(m_{AB}, \frac{m_{AB}}{\Omega_{AB}}r^2\right)}{\Gamma(m_{AB})} \tag{2.4}$$

where $\Gamma(x)$ is the Gamma function as defined in [16, eq. (8.310.1)] and $\gamma(a, b)$ is the lower incomplete gamma function as defined in [16, eq. (8.350.1)]. Note that m_{AB} and Ω_{AB} are the Nakagami parameter and the average power of the fading, respectively. Similar to Rician fading, m_{AB} is a indicator of the severity of the fading, with small m_{AB} implying severe fading and large m_{AB} implying mild fading. In addition, m_{AB} can take any value between 0.5 to ∞. When $m_{AB} = 1$, Nakagami-*m* fading reduces to Rayleigh fading and when $m_{AB} = \infty$, we have no fading. When $m_{AB} = 0.5$, the fading will be more severe than Rayleigh fading [18] [19].

Note that the mathematical expression for Rician distribution contains a Bessel function while the Nakagami-*m* distribution contains a gamma function, which is easier to manipulate mathematically. Thus, the Nakagami-*m* distribution often leads to closed-form analytical expressions that are not possible for the Rician distribution. The switching rate obtained in this thesis is one such example. Also, in the literature, the Nakagami-*m* distribution is sometimes used to approximate the Rician distribution. However, in this thesis we find that such approximation is not appropriate for switching rate, especially in switch-and-examine relaying.

2.2 Transmission Protocols

In this thesis, the terminals are assumed to be half-duplex, i.e., the terminals can receive and transmit information but are not capable of receiving and transmitting at the same time, and may operate in either the AF or the DF mode.

Two different transmission protocols are investigated. The first is opportunistic relaying, in which only the relay with the highest performance metric of L available relays is activated. In order to achieve full diversity, the performance metric must account for the channel quality of both hops. As suggested in [3], we use the minimum of the channel gains as the performance metric,

$$R_i = \min(R_{Si}, R_{iD}). \tag{2.5}$$

Therefore, the node with highest R_i is activated. This is the optimal choice for systems operating in DF mode since the weakest link explicitly determines the outage capacity. This is also an appropriate choice for systems operating in AF mode since the weakest link usually dominates the overall performance. Moreover, it is a tight upper bound of a popular performance metric, the harmonic-mean metric proposed in [20], while it is more mathematically tractable compared to the harmonic-mean metric. Note that this performance metric has been proved to achieve full diversity in opportunistic relaying systems [3], [4] and switch-and-examine systems [6].

The second scheme is switch-and-examine relaying, which is a direct extension of the switch-and-stay relaying scheme in [11] to multiple relays. Unlike opportunistic relaying, the currently active relay stays active as long as its performance metric stays above some specific level. Evidently, such a performance metric has to account for the channel quality of both hops, just like that in opportunistic relaying. Therefore, R_i is used for switch-and-examine relaying too. A switch occurs whenever the performance metric R_i of the active relaying terminal experiences a negative-going crossing of the predetermined switching threshold R_{th}, regardless of the channel conditions of other relays. This scheme avoids excessive switching when channel conditions are weak. This switching scheme is different from that adopted in [6] in which a switch occurs whenever the channel condition of the active terminal is below R_{th}. Returning to the switching scheme examined in the present thesis, note that the operation after switching depends on the value of L. If L equals 2, the destination simply communicates with the other relay until another switch occurs. If L is larger than 2, the system examines each relay in a predetermined order to activate the first relay having R_i above the switching threshold. If all the other relays are below the switching threshold, either the best relay is selected or the system selects a relay randomly. Note that while these two schemes give different error rate performances, both yield the same switching rate in i.i.d. fading.

Finally, it is assumed that the destination selects the appropriate node after performing channel estimation of all links. For simplicity, it is assumed that the destination can obtain accurate channel state information (CSI) of all links. Methods for achieving accurate channel estimation in conventional point-to-point communication systems are well known [15, Ch. 5]. In DF, the channel estimation for the overall system is simply two point-to-point channel estimations at the relay and the destination. Methods for utilizing various training sequences to obtain channel estimation in AF can be found in [21] and [22] and the references therein. Note that in OR, the destination needs to keep track of the CSI of all links at any given time, while in switch-and-examine relaying, the destination needs only the CSI of the active link if no switch occurs. When a switch does occur, the destination needs the CSI of other links, which still alleviates the burden of channel estimation compared to OR.

Chapter 3

Switching Rate of Opportunistic Relaying

In this chapter[1], we find the switching rate of opportunistic relaying systems. In order to do so, we first find the statistics of the performance metric R_i, in particular, the PDF and CDF of R_i, $f_{R_i}(r)$ and $F_{R_i}(r)$. Since R_i is the minimum of two independent random variables, R_{Si} and R_{iD}, according to order statistics [25], the PDF and CDF of R_i can be expressed as

$$f_{R_i}(r) = f_{R_{Si}}(r)\left[1 - F_{R_{iD}}(r)\right] + f_{R_{iD}}(r)\left[1 - F_{R_{Si}}(r)\right] \tag{3.1}$$

$$F_{R_i}(r) = 1 - \left[1 - F_{R_{Si}}(r)\right]\left[1 - F_{R_{iD}}(r)\right] \tag{3.2}$$

where $f_{R_{AB}}(r)$ and $F_{R_{AB}}(r)$ denote the PDF and CDF of the channel amplitude of link AB. If the system undergoes i.n.i.d Rician fading, using (2.1) and (2.2), we get

$$\begin{aligned} f_{R_i}(r) = {} & \frac{r}{\sigma_{Si}^2} \exp\left(-\frac{r^2}{2\sigma_{Si}^2} - K_{Si}\right) I_0\left(\sqrt{2K_{Si}}\frac{r}{\sigma_{Si}}\right) Q_1\left(\sqrt{2K_{iD}}, \frac{r}{\sigma_{iD}}\right) \\ & + \frac{r}{\sigma_{iD}^2} \exp\left(-\frac{r^2}{2\sigma_{iD}^2} - K_{iD}\right) I_0\left(\sqrt{2K_{iD}}\frac{r}{\sigma_{iD}}\right) Q_1\left(\sqrt{2K_{Si}}, \frac{r}{\sigma_{Si}}\right) \end{aligned} \tag{3.3}$$

$$F_{R_i}(r) = 1 - Q_1\left(\sqrt{2K_{Si}}, \frac{r}{\sigma_{Si}}\right) Q_1\left(\sqrt{2K_{iD}}, \frac{r}{\sigma_{iD}}\right). \tag{3.4}$$

Similarly, if the system undergoes i.n.i.d Nakagami-*m* fadings, using (2.3) and

[1] The results in this chapter have been presented in part at the IEEE Global Communications Conference (GLOBECOM) 2011, held in Houston, Texas, USA [23] and in part in the *IEEE Transactions on Communications* [24].

(2.4), we get

$$f_{R_i}(r) = \frac{2r^{2m_{Si}-1}}{\Gamma(m_{Si})}\left(\frac{m_{Si}}{\Omega_{Si}}\right)^{m_{Si}} \exp\left(-\frac{m_{Si}r^2}{\Omega_{Si}}\right)\frac{\Gamma\left(m_{iD}, \frac{m_{iD}}{\Omega_{iD}}r^2\right)}{\Gamma(m_{iD})} + \frac{2r^{2m_{iD}-1}}{\Gamma(m_{iD})}\left(\frac{m_{iD}}{\Omega_{iD}}\right)^{m_{iD}} \exp\left(-\frac{m_{iD}r^2}{\Omega_{iD}}\right)\frac{\Gamma\left(m_{Si}, \frac{m_{Si}}{\Omega_{Si}}r^2\right)}{\Gamma(m_{Si})} \tag{3.5}$$

$$F_{R_i}(r) = 1 - \frac{\Gamma\left(m_{Si}, \frac{m_{Si}}{\Omega_{Si}}r^2\right)}{\Gamma(m_{Si})}\frac{\Gamma\left(m_{iD}, \frac{m_{iD}}{\Omega_{iD}}r^2\right)}{\Gamma(m_{iD})} \tag{3.6}$$

where $\Gamma(a,b)$ is the upper incomplete gamma function as defined in [16, eq. (8.350.2)].

If the system undergoes i.i.d. Rician fadings with parameters K_i and σ_i, (3.3) and (3.4) will respectively reduce to

$$f_{R_i}(r) = \frac{2r}{\sigma_i^2}\exp\left(-\frac{r^2}{2\sigma_i^2} - K_i\right) I_0\left(\sqrt{2K_i}\frac{r}{\sigma_i}\right) Q_1\left(\sqrt{2K_i}, \frac{r}{\sigma_i}\right) \tag{3.7}$$

$$F_{R_1}(r) = 1 - Q_1^2\left(\sqrt{2K_i}, \frac{r}{\sigma_i}\right). \tag{3.8}$$

Similarly, for i.i.d. Nakagami-*m* fadings with parameters m_i and Ω_i, (3.5) and (3.6) will respectively reduce to

$$f_{R_i}(r) = \frac{4m_i^{m_i}r^{2m_i-1}}{\Gamma(m_i)\Omega_i^{m_i}}\exp\left(-\frac{m_ir^2}{\Omega_i}\right)\frac{\Gamma\left(m_i, \frac{m_i}{\Omega_i}r^2\right)}{\Gamma(m_i)} \tag{3.9}$$

$$F_{R_1}(r) = 1 - \frac{\Gamma^2(m_i, \frac{m_i}{\Omega_i}r^2)}{\Gamma^2(m_i)}. \tag{3.10}$$

In the sequel, K, σ, m and Ω will be used to designate values of K_i, σ_i, m_i and Ω_i when reference to the channel index is not needed.

3.1 Switching Rate of Dual-Branch i.n.i.d. Opportunistic Relaying

Now we define a random process $Z(t)$ as [8], [9]

$$Z(t) = R_1(t) - R_2(t). \tag{3.11}$$

Clearly, a positive-going zero-crossing of $Z(t)$ indicates the system switches from relay 2 to relay 1, and a negative-going zero-crossing of $Z(t)$ indicates the system switches from relay 1 to relay 2. Therefore, the total switching rate of the system equals the sum of the positive-going and negative-going zero-crossing rates of $Z(t)$, which can be expressed as [14, Ch. 2]

$$SR_{OR} = \int_{-\infty}^{0} |\dot{z}| f(0, \dot{z})\, d\dot{z} + \int_{0}^{\infty} \dot{z} f(0, \dot{z})\, d\dot{z} \tag{3.12}$$

where $f(z, \dot{z})$ denotes the joint PDF of $Z(t)$ and its time-derivative, $\dot{Z}(t)$. In many important practical cases, such as Rician and Nakagami-*m* fading under conditions detailed in [8], [14], R_{Si} and $\dot{R}_{Si}$ are independent (as are also R_{iD} and $\dot{R}_{iD}$). We assume that the required conditions are satisfied here. We also assume independence between R_{Si} and R_{iD}. Thus, we ensure the independence between R_i and $\dot{R}_i$, which leads to independence between $Z(t)$ and $\dot{Z}(t)$. Therefore $f(z, \dot{z}) = f_Z(z) f_{\dot{Z}}(\dot{z})$ where $f_Z(z)$ and $f_{\dot{Z}}(\dot{z})$ denote the PDFs of $Z(t)$ and $\dot{Z}(t)$ respectively. Then, (3.12) becomes

$$SR_{OR} = f_Z(0) \left[\int_{-\infty}^{0} |\dot{z}| f_{\dot{Z}}(\dot{z})\, d\dot{z} + \int_{0}^{\infty} \dot{z} f_{\dot{Z}}(\dot{z})\, d\dot{z} \right]. \tag{3.13}$$

We first find the value of $f_Z(0)$ for Rician and Nakagami-*m* fading. Note that $f_Z(0)$ can be evaluated as

$$f_Z(0) = \int_{0}^{\infty} f_{R_1}(r) f_{R_2}(r)\, dr. \tag{3.14}$$

By inserting (3.7) into (3.14), we obtain $f_Z(0)$ in i.i.d. Rician fading as

$$f_Z(0) = \frac{4}{\sigma_i^4} \int_{0}^{\infty} r^2 \exp\left(-\frac{r^2}{\sigma_i^2} - 2K_i \right) I_0^2 \left(\sqrt{2K_i} \frac{r}{\sigma_i} \right) Q_1^2 \left(\sqrt{2K_i}, \frac{r}{\sigma_i} \right) dr. \tag{3.15}$$

Similarly, by inserting (3.9) into (3.14), we obtain $f_Z(0)$ in i.i.d. Nakagami-*m* fading as

$$f_Z(0) = \frac{16}{\Gamma^4(m_i) \Omega_i^{2m_i}} \int_{0}^{\infty} r^{4m_i - 1} \exp\left(-\frac{2m_i r}{\Omega_i} \right) \Gamma^2 \left(m_i, \frac{m_i}{\Omega_i} r^2 \right) dr. \tag{3.16}$$

Finally, $f_Z(0)$ in i.n.i.d. Rician and Nakagami-*m* fadings can be obtained by inserting (3.3) and (3.5) into (3.14), respectively. However, the full expressions in both cases is tedious and give little insight, thus they are omitted here. The expressions for $f_Z(0)$ in i.n.i.d. fading are just more complicated versions of $f_Z(0)$ in i.i.d. fading.

The single integrals in $f_Z(0)$ can be efficiently evaluated using popular mathematics packages such as MATLAB and Mathematica. Note that the integrals in i.n.i.d. cases are very similar to those in i.i.d. cases. To the author's best knowledge, no closed-form solution to an integral similar to that in (3.15) is available. However, for Nakagami-*m* fading, we find a compact closed-form solution for an integral similar to that in (3.16) when m is an integer. Moreover, a closed-form solution expressed in terms of the hypergeometric function is available when m is not an integer. These closed-form solutions are derived in Appendix A.1 and Appendix A.2.

Now we turn our attention to the two integrals in (3.13). Observe that $\dot{Z}(t)$ equals the difference of the time derivatives $\dot{R}_1(t)$ and $\dot{R}_2(t)$. To derive the PDF of $\dot{Z}(t)$, $f_{\dot{Z}}(\dot{z})$, we need to obtain the PDF of $\dot{R}_i(t)$, $f_{\dot{R}_i}(x)$, which can be expressed as

$$f_{\dot{R}_i}(x) = p_i f_{\dot{R}_{Si}}(x) + (1-p_i) f_{\dot{R}_{iD}}(x) \tag{3.17}$$

where p_i denotes the probability that $R_{Si} \leqslant R_{iD}$ and where $f_{\dot{R}_{Si}}(x)$ and $f_{\dot{R}_{iD}}(x)$ denote the PDF of the time derivatives of R_{Si} and R_{iD}, respectively. First of all p_i can be expressed as

$$p_i = \int_0^\infty f_{R_{Si}}(x) \left[1 - F_{R_{iD}}(x)\right] \, dx. \tag{3.18}$$

For Rician fading, by substituting (2.1) and (2.2) into (3.18), we obtain

$$\begin{aligned} p_i = {} & Q_1\left(\frac{\sqrt{2K_{iD}}\sigma_{iD}}{\sqrt{\sigma_{Si}^2+\sigma_{iD}^2}}, \frac{\sqrt{2K_{Si}}\sigma_{Si}}{\sqrt{\sigma_{Si}^2+\sigma_{iD}^2}}\right) \\ & - \frac{\sigma_{Si}^2}{\sigma_{Si}^2+\sigma_{iD}^2} \exp\left[-\frac{K_{Si}\sigma_{Si}^2 + K_{iD}\sigma_{iD}^2}{\sigma_{Si}^2+\sigma_{iD}^2}\right] I_0\left(\frac{2\sqrt{K_{Si}K_{iD}}\sigma_{Si}\sigma_{iD}}{\sigma_{Si}^2+\sigma_{iD}^2}\right) \end{aligned} \tag{3.19}$$

where [17, eq. (B.32)] is used. It is easy to see that (3.19) depends only on the ratio between σ_{Si} and σ_{iD}, i.e., if $\frac{\sigma_{Si}}{\sigma_{iD}} = \alpha$, p_i only depends on α. Note that if $K_{Si} = K_{iD} = 0$, Rician fading reduces to Rayleigh fading and (3.19) reduces to $p_i = \frac{\sigma_{iD}^2}{\sigma_{Si}^2+\sigma_{iD}^2}$ (note that $Q_1(0,0) = 1$ and $I_0(0) = 1$), which agrees with the results given in [11, eq. (52)]. Also, if the channel experiences i.i.d. Rician fadings, i.e., $K_{Si} = K_{iD} = K_i$ and $\sigma_{Si} = \sigma_{iD} = \sigma_i$, by inserting these into (3.19), we have

$$p_i = Q_1\left(\sqrt{K_i}, \sqrt{K_i}\right) - \frac{1}{2}\exp\left(-K_i\right) I_0\left(K_i\right) \tag{3.20}$$

while according to [26, eq. A-3-2], $Q_1(a,a) = \frac{1}{2}\left[1+\exp(-a^2)I_0(a^2)\right]$. Therefore, we have $p_i = \frac{1}{2}$ when the channel experiences i.i.d. Rician fadings as expected.

Similarly, if the channels experience Nakagami-*m* fading, by substituting (2.3) and (2.4) into (3.18), we have

$$p_i = 1 - \left(\frac{m_{Si}}{\Omega_{Si}}\right)^{m_{Si}} \left(\frac{m_{iD}}{\Omega_{iD}}\right)^{m_{iD}} \frac{\Gamma(m_{Si}+m_{iD})}{\Gamma(m_{Si})\Gamma(m_{iD})} \cdot \frac{{}_2F_1\left(1, m_{Si}+m_{iD}; m_{iD}+1; \frac{\Omega_{Si}m_{iD}}{\Omega_{Si}m_{iD}+\Omega_{iD}m_{Si}}\right)}{m_{iD}\left(\frac{m_{Si}}{\Omega Si}+\frac{m_{iD}}{\Omega iD}\right)^{m_{Si}+m_{iD}}} \tag{3.21}$$

where ${}_2F_1(a,b;c;d)$ denotes the Gaussian hypergeometric function defined at [16, eq. (9.100)]. We employ [16, eq. (6.455.2)] to obtain (3.21). Similar to p_i in Rician fading, one can see that (3.21) depends only on the ratio between Ω_{Si} and Ω_{iD}, i.e. if $\frac{\Omega_{Si}}{\Omega_{iD}} = \alpha$, p_i only depends on α. Note that if $m_{Si} = m_{iD} = 1$, Nakagami-*m* fading reduces to Rayleigh fading. In this case, we have

$$p_i = 1 - \frac{1}{\Omega_{Si}}\frac{1}{\Omega_{iD}}\frac{{}_2F_1\left(1,2;2;\frac{\Omega_{Si}}{\Omega_{Si}+\Omega_{iD}}\right)}{\left(\frac{1}{\Omega Si}+\frac{1}{\Omega iD}\right)^2}. \tag{3.22}$$

According to [16, eq. (9.121.1)], we have ${}_2F_1(-n,\beta;\beta;-z) = (1+z)^n$. Using this identity and some simple manipulation, we will have $p_i = \frac{\Omega_{iD}}{\Omega_{Si}+\Omega_{iD}}$, which again agrees with [11, eq. (52)]. Also, if the channel experiences i.i.d. Nakagami-*m* fadings, i.e., $m_{Si} = m_{iD} = m_i$ and $\Omega_{Si} = \Omega_{iD} = \Omega_i$, it can be shown that $p_i = \frac{1}{2}$. The detailed proof is the following. Applying the i.i.d. assumption, we can simplify (3.21) as

$$\begin{aligned} p_i &= 1 - \frac{\Gamma(2m_i)}{\Gamma^2(m_i)}\frac{{}_2F_1(1,2m_i;m_i+1;0.5)}{m_i 2^{2m_i}} && (3.23)\\ &= 1 - \frac{\Gamma(2m_i)}{\Gamma^2(m_i)}\frac{{}_2F_1(0.5,m_i;m_i+1;1)}{m_i 2^{2m_i}} && (3.24)\\ &= 1 - \frac{\Gamma(2m_i)}{\Gamma^2(m_i)}\frac{\Gamma(m_i+1)\Gamma(0.5)}{\Gamma(m_i+0.5)m_i 2^{2m_i}} && (3.25)\\ &= 1 - \frac{2^{2m_i-1}\Gamma(m_i)\Gamma(m_i+0.5)}{\Gamma^2(m_i)}\frac{m_i\Gamma(m_i)}{m_i\Gamma(m_i+0.5)2^{2m_i}} && (3.26)\\ &= \frac{1}{2}. && (3.27) \end{aligned}$$

Note that we obtain (3.24) by using [16, eq. (9.133)], obtain (3.25) by using [16, eq. (9.122.1)], obtain (3.26) by using [16, eq. (8.335.1)] together with some well known identities involving the Gamma function, such as $\Gamma(0.5) = \sqrt{\pi}$ and $\Gamma(m+1) = m\Gamma(m)$.

Secondly, $f_{\dot{R}_{AB}}(x)$ can be expressed as

$$f_{\dot{R}_{AB}}(x) = \frac{1}{\sqrt{2\pi}\dot{\sigma}_{AB}} \exp(-\frac{x^2}{2\dot{\sigma}_{AB}^2}). \tag{3.28}$$

For Rician fading [14, Ch. 2],

$$\dot{\sigma}_{AB} = \sqrt{2}\pi f_{AB}\sigma_{AB} \tag{3.29}$$

and for Nakagami-*m* fading [27],

$$\dot{\sigma}_{AB} = \pi f_{AB}\sqrt{\frac{\Omega_{AB}}{m_{AB}}}. \tag{3.30}$$

Note that $f_{\dot{R}_{Si}}(x)$ and $f_{\dot{R}_{iD}}(x)$ are both zero-mean Gaussian PDFs with standard deviations $\dot{\sigma}_{Si}$ and $\dot{\sigma}_{iD}$, respectively. Since $\dot{Z}(t) = \dot{R}_1(t) - \dot{R}_1(t)$, the PDF of $\dot{Z}(t)$, $f_{\dot{Z}}(x)$ is

$$\begin{aligned}
f_{\dot{Z}}(x) &= \int_{-\infty}^{\infty} f_{\dot{R}_1}(y+x) f_{\dot{R}_2}(y)\, dy & (3.31)\\
&= \frac{p_1 p_2}{\sqrt{2\pi(\dot{\sigma}_{S1}^2 + \dot{\sigma}_{S2}^2)}} \exp\left(-\frac{x^2}{2(\dot{\sigma}_{S1}^2 + \dot{\sigma}_{S2}^2)}\right)\\
&+ \frac{p_1(1-p_2)}{\sqrt{2\pi(\dot{\sigma}_{S1}^2 + \dot{\sigma}_{2D}^2)}} \exp\left(-\frac{x^2}{2(\dot{\sigma}_{S1}^2 + \dot{\sigma}_{2D}^2)}\right)\\
&+ \frac{(1-p_1)p_2}{\sqrt{2\pi(\dot{\sigma}_{1D}^2 + \dot{\sigma}_{S2}^2)}} \exp\left(-\frac{x^2}{2(\dot{\sigma}_{1D}^2 + \dot{\sigma}_{S2}^2)}\right)\\
&+ \frac{(1-p_1)(1-p_2)}{\sqrt{2\pi(\dot{\sigma}_{1D}^2 + \dot{\sigma}_{2D}^2)}} \exp\left(-\frac{x^2}{2(\dot{\sigma}_{1D}^2 + \dot{\sigma}_{2D}^2)}\right). & (3.32)
\end{aligned}$$

After some straightforward integration it can be shown that

$$\begin{aligned}
&\int_0^{\infty} \dot{z} f_{\dot{Z}}(\dot{z})\, d\dot{z} = \int_{-\infty}^{0} |\dot{z}| f_{\dot{Z}}(\dot{z})\, d\dot{z}\\
&= \frac{1}{\sqrt{2\pi}} p_1 p_2 \sqrt{\dot{\sigma}_{S1}^2 + \dot{\sigma}_{S2}^2} + \frac{1}{\sqrt{2\pi}}(1-p_1)(1-p_2)\sqrt{\dot{\sigma}_{1D}^2 + \dot{\sigma}_{2D}^2}\\
&+ \frac{1}{\sqrt{2\pi}} p_1(1-p_2)\sqrt{\dot{\sigma}_{S1}^2 + \dot{\sigma}_{2D}^2} + \frac{1}{\sqrt{2\pi}}(1-p_1)p_2\sqrt{\dot{\sigma}_{1D}^2 + \dot{\sigma}_{S2}^2}. \qquad (3.33)
\end{aligned}$$

For a network experiencing i.i.d. fadings with the same Doppler shift, $p_1 = p_2 = 0.5$ and $\dot{\sigma}_{S1} = \dot{\sigma}_{S2} = \dot{\sigma}_{1D} = \dot{\sigma}_{2D} = \dot{\sigma}$, (3.33) reduces to

$$\int_0^\infty \dot{z} f_{\dot{Z}}(\dot{z})\, d\dot{z} = \int_{-\infty}^0 |\dot{z}| f_{\dot{Z}}(\dot{z})\, d\dot{z} = \frac{\dot{\sigma}}{\sqrt{\pi}}. \tag{3.34}$$

In summary, the switching rate is

$$SR_{OR} = 2 f_Z(0) \int_0^\infty \dot{z} f_{\dot{Z}}(\dot{z})\, d\dot{z}. \tag{3.35}$$

For i.n.i.d. Rician fading, we have

$$f_Z(0) = \int_0^\infty f_{R_1}(r) f_{R_2}(r)\, dr \tag{3.36a}$$

where $f_{R_i}(r)$ is given by

$$\begin{aligned} f_{R_i}(r) = &\frac{r}{\sigma_{Si}^2} \exp\left(-\frac{r^2}{2\sigma_{Si}^2} - K_{Si}\right) I_0\left(\sqrt{2K_{Si}}\frac{r}{\sigma_{Si}}\right) Q_1\left(\sqrt{2K_{iD}}, \frac{r}{\sigma_{iD}}\right) \\ &+ \frac{r}{\sigma_{iD}^2} \exp\left(-\frac{r^2}{2\sigma_{iD}^2} - K_{iD}\right) I_0\left(\sqrt{2K_{iD}}\frac{r}{\sigma_{iD}}\right) Q_1\left(\sqrt{2K_{Si}}, \frac{r}{\sigma_{Si}}\right). \end{aligned} \tag{3.36b}$$

In addition, $\int_0^\infty \dot{z} f_{\dot{Z}}(\dot{z})\, d\dot{z}$ are given in (3.33) with

$$\begin{aligned} p_i = &Q_1\left(\frac{\sqrt{2K_{iD}}\sigma_{iD}}{\sqrt{\sigma_{Si}^2 + \sigma_{iD}^2}}, \frac{\sqrt{2K_{Si}}\sigma_{Si}}{\sqrt{\sigma_{Si}^2 + \sigma_{iD}^2}}\right) \\ &- \frac{\sigma_{Si}^2}{\sigma_{Si}^2 + \sigma_{iD}^2} \exp\left[-\frac{K_{Si}\sigma_{Si}^2 + K_{iD}\sigma_{iD}^2}{\sigma_{Si}^2 + \sigma_{iD}^2}\right] I_0\left(\frac{2\sqrt{K_{Si}K_{iD}}\sigma_{Si}\sigma_{iD}}{\sigma_{Si}^2 + \sigma_{iD}^2}\right) \end{aligned} \tag{3.37a}$$

$$\dot{\sigma}_{AB} = \sqrt{2}\pi f_{AB} \sigma_{AB}. \tag{3.37b}$$

For i.n.i.d. Nakagami-*m* fading, $f_{R_i}(r)$, p_i and $\dot{\sigma}_{AB}$ are given by

$$\begin{aligned} f_{R_i}(r) = &\frac{2r^{2m_{Si}-1}}{\Gamma(m_{Si})}\left(\frac{m_{Si}}{\Omega_{Si}}\right)^{m_{Si}} \exp\left(-\frac{m_{Si}r^2}{\Omega_{Si}}\right) \frac{\Gamma\left(m_{iD}, \frac{m_{iD}}{\Omega_{iD}}r^2\right)}{\Gamma(m_{iD})} \\ &+ \frac{2r^{2m_{iD}-1}}{\Gamma(m_{iD})}\left(\frac{m_{iD}}{\Omega_{iD}}\right)^{m_{iD}} \exp\left(-\frac{m_{iD}r^2}{\Omega_{iD}}\right) \frac{\Gamma\left(m_{Si}, \frac{m_{Si}}{\Omega_{Si}}r^2\right)}{\Gamma(m_{Si})} \end{aligned} \tag{3.38a}$$

$$\begin{aligned} p_i = 1 - &\left(\frac{m_{Si}}{\Omega_{Si}}\right)^{m_{Si}} \left(\frac{m_{iD}}{\Omega_{iD}}\right)^{m_{iD}} \frac{\Gamma(m_{Si} + m_{iD})}{\Gamma(m_{Si})\Gamma(m_{iD})} \\ &\cdot \frac{{}_2F_1\left(1, m_{Si} + m_{iD}; m_{iD} + 1; \frac{\Omega_{Si}m_{iD}}{\Omega_{Si}m_{iD} + \Omega_{iD}m_{Si}}\right)}{m_{iD}\left(\frac{m_{Si}}{\Omega Si} + \frac{m_{iD}}{\Omega iD}\right)^{m_{Si}+m_{iD}}} \end{aligned} \tag{3.38b}$$

$$\dot{\sigma}_{AB} = \pi f_{AB}\sqrt{\frac{\Omega_{AB}}{m_{AB}}}. \tag{3.38c}$$

Thus, by inserting (3.37) into (3.33), we have the full expression of $\int_0^\infty \dot{z} f_{\dot{Z}}(\dot{z})\, d\dot{z}$. At the same time, we obtain full expression of $f_Z(0)$ by using (3.36). Inserting these two results into (3.35), we obtain the switching rate for dual-branch OR with i.n.i.d. Rician fading. Following the same procedure, but using equations in (3.38) instead, we obtain the switching rate for dual-branch OR with i.n.i.d. Nakagami-*m* fading. The exact expressions are unwieldy and gives little insight, thus they are omitted. For i.i.d cases, the expression is much more compact. For i.i.d. Rician fadings with identical maximum Doppler shift, f_m, the switching rate is

$$SR_{OR} = \frac{8\sqrt{2\pi} f_m}{\sigma^3}\int_0^\infty r^2 \exp\left(-\frac{r^2}{\sigma^2} - 2K\right) I_0^2\left(\sqrt{2K}\frac{r}{\sigma}\right) Q_1^2\left(\sqrt{2K}, \frac{r}{\sigma}\right)\, dr. \tag{3.39}$$

Close inspection reveals that SR_{OR} does not depend on σ alone. To see this, one could replace r with $r\sigma$ and σ will be canceled out. In fact, this is not limited to i.i.d. fading. In i.n.i.d. fading, the switching rate depends only on the relative relationships between σ_{S1}, σ_{1D}, σ_{S2}, and σ_{2D}. Specifically, if $\sigma_{S1} = \sigma$, $\sigma_{1D} = \alpha\sigma$, $\sigma_{S2} = \beta\sigma$ and $\sigma_{2D} = \gamma\sigma$ the switching rate depends only on α, β and γ but not σ. Therefore, SR_{OR} can be rewritten as

$$SR_{OR} = 8\sqrt{2\pi} f_m \int_0^\infty r^2 \exp\left(-r^2 - 2K\right) I_0^2\left(\sqrt{2K} r\right) Q_1^2\left(\sqrt{2K}, r\right)\, dr. \tag{3.40}$$

Note that the switching rate grows linearly with f_m.

For system experiencing i.i.d. Nakagami-*m* fadings with identical maximum Doppler shifts f_m, the switching rate is

$$SR_{OR} = \frac{32\sqrt{\pi} f_m}{\Gamma^4(m)}\left(\frac{m}{\Omega}\right)^{2m-\frac{1}{2}}\int_0^\infty r^{4m-2} \exp\left(-\frac{2mr^2}{\Omega}\right) \Gamma^2\left(m, \frac{m}{\Omega} r^2\right)\, dr. \tag{3.41}$$

Similar to Rician fading, the switching rate does not depend on Ω alone. To see this, one could replace r with $r\sqrt{\Omega}$ and then Ω will be canceled out. The switching rate in the i.n.i.d. case also depends only on the relative relationships between Ω_{S1}, Ω_{1D}, Ω_{S2} and Ω_{2D}. Therefore, SR_{OR} can be rewritten as

$$SR_{OR} = \frac{32\sqrt{\pi} f_m}{\Gamma^4(m)} m^{2m-\frac{1}{2}}\int_0^\infty r^{4m-2} \exp\left(-2mr^2\right) \Gamma^2\left(m, mr^2\right)\, dr. \tag{3.42}$$

The switching rate again grows linearly with f_m.

For Nakagami-*m* fading, the integral in (3.42) has closed-form solutions. If m is an integer, by using (A.5), the switching rate reduces to

$$SR_{OR} = \frac{2f_m\sqrt{\pi}}{4^{2m-2}\Gamma^2(m)} \sum_{i=0}^{m-1} \sum_{j=0}^{m-1} \frac{\Gamma(i+j+2m-0.5)}{i!j!4^{i+j}}. \tag{3.43}$$

If m is not an integer, by using (A.8) the switching rate is

$$\begin{aligned} SR_{OR} = \frac{32\sqrt{\pi}f_m}{\Gamma^4(m)} & \left[\frac{\Gamma(4m-\frac{1}{2})}{4^{4m-\frac{1}{2}}m^2} F_2(4m-\frac{1}{2}, 1, 1, 1+m, 1+m; \frac{1}{4}, \frac{1}{4}) \right. \\ & \left. -2\Gamma(m)\frac{\Gamma(3m-\frac{1}{2})}{3^{3m-\frac{1}{2}}m} {}_2F_1(1, 3m-\frac{1}{2}; m+1; \frac{1}{3}) + \Gamma^2(m)\frac{\Gamma(2m-\frac{1}{2})}{2^{2m-\frac{1}{2}}} \right]. \end{aligned} \tag{3.44}$$

where $F_2(\alpha, \beta, \beta', \gamma, \gamma'; x, y)$ is the hypergeometric function of two variables and is given in (A.9).

In the next section, we derive the switching rate of multi-branch OR with i.i.d. fadings.

3.2 Switching Rate of Multi-Branch i.i.d. Case

For multi-branch systems, the switching rate can be expressed as

$$SR_{OR} = \sum_{i=1}^{L} SR_{OR,i} \tag{3.45}$$

where $SR_{OR,i}$ is the rate at which the system switches to R_i from any other relays. Similar to the development in the previous section, we define a new random process

$$Z_i(t) = R_i(t) - \max_{\substack{j\in\{1,\dots,L\} \\ j\neq i}} R_j(t). \tag{3.46}$$

Obviously, $SR_{OR,i}$ equals the positive-going zero-crossing rate of $Z_i(t)$. Employing the same approach as in the previous section, we can evaluate $SR_{OR,i}$ for every i, and then obtain SR_{OR}. However, the expression for an i.n.i.d multi-branch system with an arbitrary number of relays is very cumbersome, therefore we only consider the i.i.d. case. Specifically, we consider a system with identical maximum

Doppler shifts f_m experiencing either Rician fading (with parameters K and σ) or Nakagami-*m* fading (with parameters m and Ω). Due to symmetry, we have

$$SR_{OR} = L \cdot SR_{OR,i}, \ \forall i \in \{1, ..., L\}. \tag{3.47}$$

Without loss of generality, we evaluate $SR_{OR,1}$ using the random process

$$Z_1(t) = R_1(t) - \max_{j \in \{2,\dots,L\}} R_j(t). \tag{3.48}$$

Similar to the dual-branch case, $SR_{OR,1}$ can be expressed as

$$SR_{OR,1} = f_{Z_1}(0) \int_0^{\infty} \dot{z} f_{\dot{Z}_1}(\dot{z})\, d\dot{z} \tag{3.49}$$

where $f_{Z_1}(z)$ and $f_{\dot{Z}_1}(z)$ denote the PDF of $Z_1(t)$ and its time-derivative $\dot{Z}_1(t)$, respectively. Using the same logic as in dual branch cases, and again assuming that the conditions required in [8], [14] are satisfied, $Z_1(t)$ and $\dot{Z}_1(t)$ are independent random processes.

Now we evaluate the integral in (3.49). First, let $f_{\dot{R}_1}(r)$ and $f_{\dot{R}_{\max}}(r)$ denote the PDFs of the time-derivative of $R_1(t)$ and $\max_{j \in \{2,\dots,L\}} R_j(t)$, respectively. Due to the i.i.d. assumption,

$$f_{\dot{R}_1}(r) = \frac{1}{2} f_{\dot{R}_{S1}}(x) + \frac{1}{2} f_{\dot{R}_{1D}}(x) = \frac{1}{\sqrt{2\pi}\dot{\sigma}} \exp(-\frac{x^2}{2\dot{\sigma}^2}) \tag{3.50}$$

where $\dot{\sigma}$ is defined in (3.29) or (3.30). Also, $f_{\dot{R}_{\max}}(r)$ is obtained as

$$f_{\dot{R}_{\max}}(r) = \sum_{k=2}^{L} \frac{1}{L-1} f_{\dot{R}_k}(r) = \frac{1}{\sqrt{2\pi}\dot{\sigma}} \exp(-\frac{x^2}{2\dot{\sigma}^2}). \tag{3.51}$$

Note that $f_{\dot{R}_1}(r)$ and $f_{\dot{R}_{\max}}(r)$ are identical Gaussian PDFs with variance $\dot{\sigma}^2$. Since $\dot{Z}_1(t)$ is the difference of two i.i.d. Gaussian random variables, $\dot{Z}_1(t)$ is also a Gaussian random variable with variance $2\dot{\sigma}^2$, and its PDF is given by

$$f_{\dot{Z}_1}(r) = \frac{1}{2\sqrt{\pi}\dot{\sigma}} \exp(-\frac{x^2}{4\dot{\sigma}^2}). \tag{3.52}$$

Therefore

$$\int_0^{\infty} \dot{z} f_{\dot{Z}_1}(\dot{z})\, d\dot{z} = \frac{\dot{\sigma}}{\sqrt{\pi}}. \tag{3.53}$$

Now we turn our attention to $f_{Z_1}(0)$, which is given by

$$f_{Z_1}(0) = \int_0^\infty f_{R_1}(r) f_{R_{\max}}(r)\, dr \tag{3.54}$$

where $f_{R_1}(r)$ and $f_{R_{\max}}(r)$ are the PDFs of $R_1(t)$ and $\max_{j\in\{2,\ldots,L\}} R_j(t)$, respectively. According to order statistics, $f_{R_{\max}}(r)$ can be expressed in terms of $f_{R_1}(r)$ as

$$f_{R_{\max}}(r) = (L-1) f_{R_1}(r) [F_{R_1}(r)]^{L-2}. \tag{3.55}$$

After some algebra manipulation, the final expression for the switching rate in Rician fading is given by

$$\begin{aligned} SR_{OR} &= 4L(L-1)\sqrt{2\pi} f_m \int_0^\infty r^2 \exp\left(-r^2 - 2K\right) \\ &\cdot I_0^2\left(\sqrt{2K}r\right) Q_1^2\left(\sqrt{2K}, r\right)\left[1 - Q_1^2(\sqrt{2K}, r)\right]^{L-2} dr. \end{aligned} \tag{3.56}$$

Unfortunately, no closed-form solution is available for the integral in (3.56). Similarly, the switching rate in Nakagami-*m* fading is given by

$$\begin{aligned} SR_{OR} &= \sqrt{\pi} f_m \frac{16L(L-1)}{\Gamma^2(m)} m^{2m-\frac{1}{2}} \int_0^\infty r^{4m-2} \exp\left(-2mr^2\right) \\ &\cdot \frac{\Gamma^2\left(m, mr^2\right)}{\Gamma^2(m)} \left[1 - \frac{\Gamma^2(m, mr^2)}{\Gamma^2(m)}\right]^{L-2} dr. \end{aligned} \tag{3.57}$$

A closed-form solution for the integral in (3.57) is derived in Appendix B. If m is an integer, with the help of Appendix B.1, an exact expression for the switching rate is found as

$$\begin{aligned} SR_{OR} &= \sqrt{\pi} f_m \frac{8L(L-1)}{\Gamma^2(m)} \sum_{i=0}^{L-2} \binom{L-2}{i} (-1)^i \\ &\cdot \sum_{\substack{k_0, k_1, \ldots, k_{m-1} \\ k_0+\ldots+k_{m-1}=2i+2}} \frac{\Gamma(\mu)}{(4+2i)^\mu} \binom{2i+2}{k_0, k_1, \ldots, k_{m-1}} \prod_{l=0}^{m-1} \left(\frac{1}{l!}\right)^{k_l} \end{aligned} \tag{3.58a}$$

with

$$\binom{n}{k_0, k_1, \ldots, k_{m-1}} = \frac{n!}{k_0! k_1! \cdots k_{m-1}!} \tag{3.58b}$$

$$\mu = \sum_{i=0}^{m-1} i k_i + 2m - 0.5. \tag{3.58c}$$

Note that in Appendix B.1, we prove that this result reduces to our previous results for the dual-branch cases when $L = 2$.

If m is not an integer, a closed-form solution is also derived as

$$SR_{OR} = \sqrt{\pi} f_m \frac{8L(L-1)}{\Gamma^{2L}(m)} \left[\Gamma^2(m) \sum_{i=0}^{L-2} c_i g(m, L-2+i) \right.$$
$$\left. -2\Gamma(m) \sum_{i=0}^{L-2} c_i g(m, L-1+i) + \sum_{i=0}^{L-2} c_i g(m, L+i) \right] \tag{3.59a}$$

with

$$c_i = \binom{L-2}{i} [2\Gamma(m)]^{L-2-i} (-1)^i. \tag{3.59b}$$

$$g(m,s) = \frac{(m)^{ms} \Gamma(2m + sm - \frac{1}{2})}{m^s [2m + sm]^{2m+sm-\frac{1}{2}}}$$
$$\cdot F_A \left(2m + sm - \frac{1}{2}; \underbrace{1, \ldots, 1}_{s \text{ terms}}; \underbrace{1+m, \ldots, 1+m}_{s \text{ terms}}; \underbrace{\frac{1}{2+s}, \ldots, \frac{1}{2+s}}_{s \text{ terms}} \right) \tag{3.59c}$$

where $F_A(\cdot;\cdot;\cdot;\cdot)$ is Lauricella's hypergeometric function of several variables and is given in Appendix B.2. As previously, when $L = 2$, the expressions reduce to the dual-branch cases. Also, as in the dual-branch cases, the switching rates grow linearly with the maximum Doppler shift f_m.

Chapter 4

Switching Rate of Switch-and-Examine Relaying

Building on the results in previous chapters, we consider the switching rate of switch-and-examine relaying in this chapter[1]. Specifically, we will derive the switching rate in closed-form.

For a switch-and-examine system with L relays, the overall switching rate SR_{swi} is

$$SR_{\text{swi}} = \sum_{i=1}^{L} \rho_i SR_{\text{swi},i} \tag{4.1}$$

where ρ_i denotes the steady-state probability that T_i is active, and $SR_{\text{swi},i}$ is the switching rate of T_i. For dual-branch (i.e., $L = 2$) systems with i.n.i.d. channel conditions, ρ_i can be derived with the help of [12, eq. (21)]. In particular, such systems have six Markov states. State 1 represents the scenario where T_1 is active and R_1 experiences a negative-going crossing of R_{th}. State 2 represents the scenario where T_1 is active and R_1 is below R_{th} for two time samples. State 3 represents the scenario where T_1 is active and R_1 is greater than R_{th} for two time samples. States 4, 5, 6 are defined in a similar fashion as states 1, 2, 3 with all indices changed to 2. The stationary probabilities, $\pi_j, j \in \{1, ..., 6\}$, are given in [12, eq. (21)] as[2]

$$\pi_1 = \frac{(1-q_1)q_1(1-q_2)q_2}{(q_1+q_2)(1+2q_1q_2) - (q_1+q_2)^2 - 2q_1^2q_2^2} \tag{4.2a}$$

[1] The results in this chapter have been presented in part at the European Wireless Conference 2011, held in Vienna, Austria [28] and in part in the *IEEE Transactions on Communications* [24].

[2] Note that there is a typographical error in the last term of [12, eq. (21)].

$$\pi_2 = \frac{q_1^2 q_2(1-q_2)}{(q_1+q_2)(1+2q_1q_2)-(q_1+q_2)^2-2q_1^2q_2^2} \tag{4.2b}$$

$$\pi_3 = \frac{(1-q_1)^2(1-q_2)q_2}{(q_1+q_2)(1+2q_1q_2)-(q_1+q_2)^2-2q_1^2q_2^2} \tag{4.2c}$$

$$\pi_4 = \frac{(1-q_1)q_1(1-q_2)q_2}{(q_1+q_2)(1+2q_1q_2)-(q_1+q_2)^2-2q_1^2q_2^2} \tag{4.2d}$$

$$\pi_5 = \frac{q_1 q_2^2(1-q_1)}{(q_1+q_2)(1+2q_1q_2)-(q_1+q_2)^2-2q_1^2q_2^2} \tag{4.2e}$$

$$\pi_6 = \frac{q_1(1-q_1)(1-q_2)^2}{(q_1+q_2)(1+2q_1q_2)-(q_1+q_2)^2-2q_1^2q_2^2} \tag{4.2f}$$

where $q_1 = F_{R_1}(R_{th})$ and $q_2 = F_{R_2}(R_{th})$. Since T_1 is active in states 1, 2, 3, while T_2 is active in states 4, 5, 6, ρ_1 and ρ_2 are given by

$$\rho_1 = \sum_{i=1}^{3} \pi_i = \frac{(1-q_1+q_1^2)(1-q_2)q_2}{(q_1+q_2)(1+2q_1q_2)-(q_1+q_2)^2-2q_1^2q_2^2} \tag{4.3}$$

$$\rho_2 = \sum_{i=4}^{6} \pi_i = \frac{(1-q_2+q_2^2)(1-q_1)q_1}{(q_1+q_2)(1+2q_1q_2)-(q_1+q_2)^2-2q_1^2q_2^2}. \tag{4.4}$$

Note that if the system experiences i.i.d. fading, $q_1 = q_2 = q$, and we have

$$\rho_1 = \rho_2 = \frac{(1-q+q^2)(1-q)q}{(2q)(1+2q^2)-(2q)^2-2q^4} = \frac{1}{2}. \tag{4.5}$$

Due to symmetry, this result is expected.

If the system has more than two branches, the expressions for ρ_i in the i.n.i.d. case with an arbitrary number of relays will be very complicated. Therefore, we only consider systems with i.i.d. fadings, where $\rho_i = \frac{1}{L}$ due to symmetry.

For relay T_i, its switching rate $SR_{\text{swi},i}$ is the rate at which the channel condition R_i will have a negative-going crossing of switching threshold R_{th}. According to the theory of level-crossing rates [14, Ch. 2], $SR_{\text{swi},i}$, is given by

$$SR_{\text{swi},i} = \int_{-\infty}^{0} |r| f_{R_i,\dot{R}_i}(R_{th}, r)\, dr \tag{4.6}$$

where $f_{R_i,\dot{R}_i}(a,b)$ is the joint PDF of R_i and its time-derivative, $\dot{R}_i$. As in the previous section, the fading process and the time-derivative process are considered independent, which guarantees the independence of R_i and $\dot{R}_i$. Therefore (4.6) reduces to

$$SR_{\text{swi},i} = f_{R_i}(R_{th}) \int_{-\infty}^{0} |r| f_{\dot{R}_i}(r)\, dr \tag{4.7}$$

where $f_{R_i}(r)$ is given in (3.3) or (3.5), depending on the fading model. Also, $f_{\dot{R}_i}(r)$ was found in the previous section; after some straightforward manipulations, it can be shown that

$$\int_{-\infty}^{0} |r| f_{\dot{R}_i}(r)\, dr = p_i \frac{\dot{\sigma}_{Si}}{\sqrt{2\pi}} + (1-p_i)\frac{\dot{\sigma}_{iD}}{\sqrt{2\pi}}. \tag{4.8}$$

We can now write the expression for the switching rate of dual-branch i.n.i.d switch-and-stay relaying as

$$SR_{\text{swi}} = \sum_{i=1}^{2} \frac{\rho_i}{\sqrt{2\pi}} f_{R_i}(R_{th}) \left[p_i \dot{\sigma}_{Si} + (1-p_i)\dot{\sigma}_{iD}\right] \tag{4.9}$$

where ρ_i is given in (4.3) and (4.4), and $f_{R_i}(r)$ is given in (3.3) or (3.5).

For multi-branch i.i.d. cases, the switching rate of networks with L relays is

$$SR_{\text{swi}} = \frac{\dot{\sigma}}{\sqrt{2\pi}} f_{R_i}(R_{th}). \tag{4.10}$$

Specifically, for systems experiencing i.i.d. Rician fadings with parameters K and σ and maximum Doppler shift f_m, we have

$$SR_{\text{swi}} = f_m \frac{2\sqrt{\pi} R_{th}}{\sigma} \exp\left(-\frac{R_{th}^2}{2\sigma^2} - K\right) I_0\left(\sqrt{2K}\frac{R_{th}}{\sigma}\right) Q_1\left(\sqrt{2K}, \frac{R_{th}}{\sigma}\right) \tag{4.11}$$

and for systems experiencing i.i.d. Nakagami-*m* fadings with parameters m and Ω and maximum Doppler shift f_m, we have

$$SR_{\text{swi}} = f_m \frac{4\sqrt{\pi} R_{th}^{2m-1}}{\Gamma(m)} \left(\frac{m}{\Omega}\right)^{m-\frac{1}{2}} \exp\left(-\frac{mR_{th}^2}{\Omega}\right) \frac{\Gamma\left(m, \frac{m}{\Omega}R_{th}^2\right)}{\Gamma(m)}. \tag{4.12}$$

If $K_i = 0$ or $m_i = 1$, Rician fading and Nakagami-*m* fading both reduce to Rayleigh fading, and (4.11) and (4.12) will coincide with the expression given in [11, eq. (42)]. Note that the switching rates in both fadings grow linearly with the maximum Doppler shift. Moreover, they depend strongly on the switching threshold, R_{th}. It is also pointed out in [6] that the choice of R_{th} affects the bit error rate (BER) strongly. While a complete treatment of the exact relation between switching rate and BER is beyond the scope of this thesis, a numerical example is provided to illuminate this relation.

Finally, note importantly that the switching rates do not depend on L. Also note that in contrast the switching rate of multi-branch opportunistic relaying depends on L (see (3.56) and (3.57)). It is shown in Chapter 5 that the switching rate of opportunistic relaying increases with L. This is not surprising, since the more relays a system has, the more frequently that the system will switch to utilize the best relay. This finding means that as a system has more relays, it is more attractive to use switch-and-examine relaying from a switching rate standpoint.

Chapter 5

Numerical Examples and Discussion

In this chapter[1], numerical examples are presented to illustrate the theoretical results. Specifically, we compare the switching rates of opportunistic relaying and switch-and-examine relaying in i.i.d. fadings. Then, we use a simulation to investigate the relation between bit error rate and switching rate. Finally, the switching rates in multi-branch systems and unbalanced systems (i.n.i.d. fading) are also investigated.

5.1 Switching Rate Comparison in i.i.d. Fading

Fig. 5.1 shows the switching rates normalized by the maximum Doppler shift, f_m, vs the threshold levels R_{th} of dual-branch opportunistic relaying and switch-and-stay relaying in i.i.d. Rician fading for different values of K with $\sigma = 1$. Fig. 5.2 shows similar results for the case of Nakagami fading with $\Omega = 2$. As expected, OR switches more frequently than does switch-and-stay relaying. The former switches 2.07, 2.10, 2.03, 2.05 and 2.01 times as frequently as the maximum rate of the latter for $K = 0, 1, 3, 7$ and 10, respectively in Rician fading. In Nakagami-*m* fading, the switching rate of OR is 1.74, 2.07, 2.03, 2.08 and 2.00 times that of the maximum switching rate of switch-and-examine relaying. Note that by changing the switching threshold of switch-and-examine relaying, the ratio of the two switching rates can

[1]The results in this chapter have been presented in part at the IEEE Global Communications Conference (GLOBECOM) 2011, held in Houston, Texas, USA [23], in part at the European Wireless Conference 2011, held in Vienna, Austra [28] and in part in the *IEEE Transactions on Communications* [24].

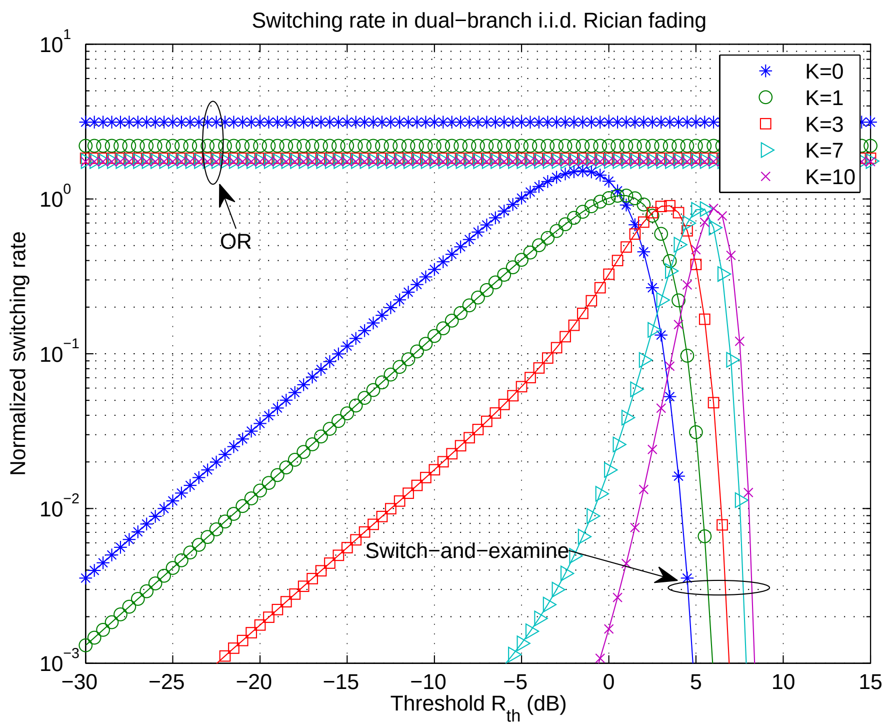

Figure 5.1. The normalized switching rates of opportunistic relaying and switch-and-examine relaying in i.i.d. Rician fading channels for different values of K with $\sigma = 1$.

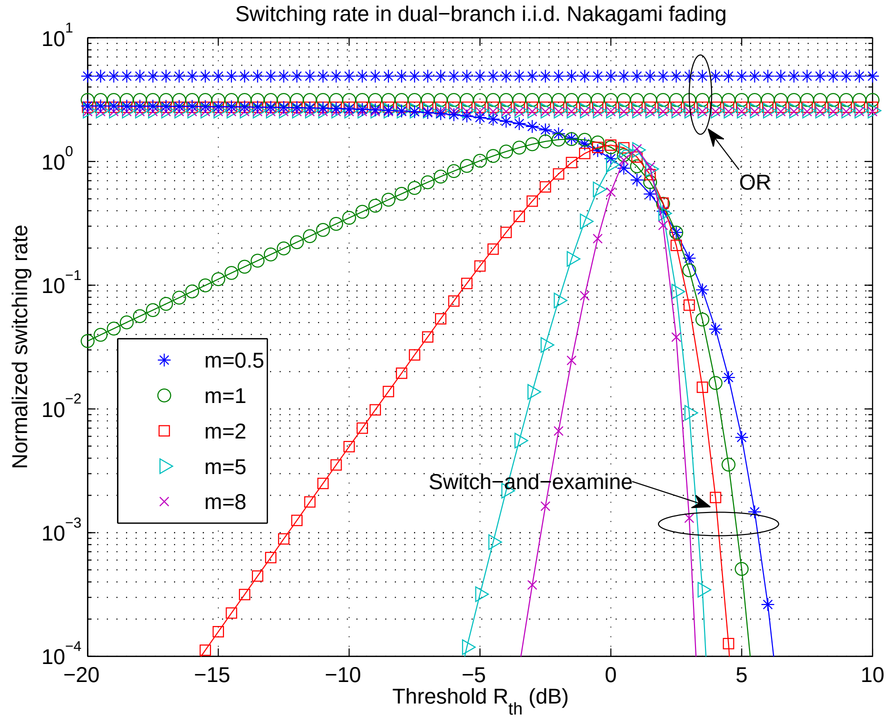

Figure 5.2. The normalized switching rates of opportunistic relaying and switch-and-examine relaying in i.i.d. Nakagami-*m* fading channels for different values of m with $\Omega = 2$.

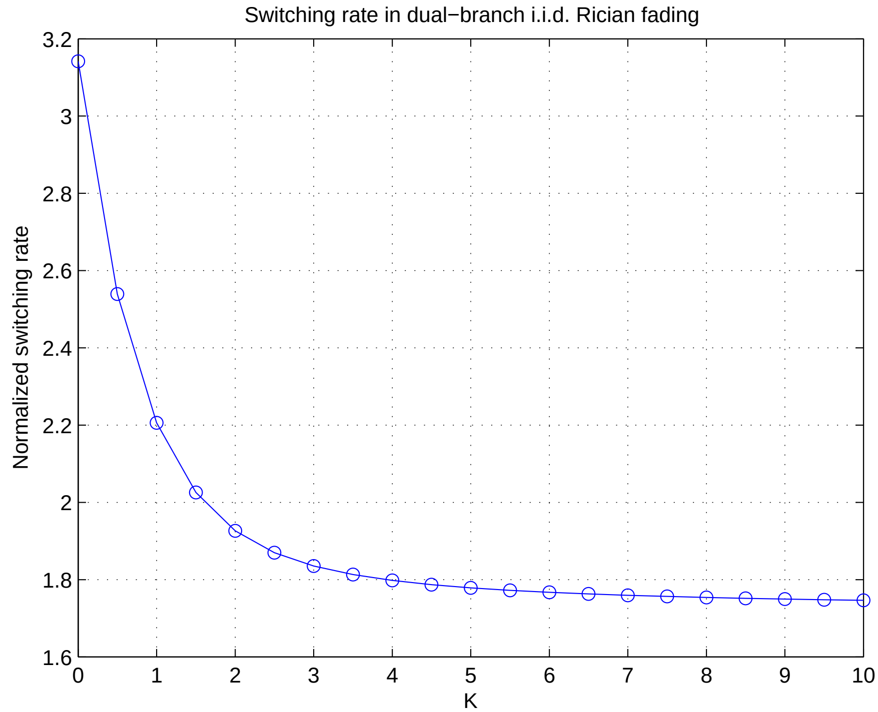

Figure 5.3. The normalized switching rates of opportunistic relaying in i.i.d. Rician fading channels for different values of σ.

be dramatically increased. Observe that as K and m become larger, the maximum switching rates of switch-and-examine relaying become smaller with diminishing increases. Also the switching rate curves compress and tend to an impulse. In the case of Rician fading, this is because as K becomes larger, the line-of-sight component of the fading process becomes more significant, and the channel amplitudes fluctuate less. In the case of Nakagami fading, as m increases, the fading becomes more shallow and again the channel amplitudes vary less.

5.2 Switching Rate of Opportunistic Relaying

Fig. 5.3 and Fig. 5.4 show the switching rates of OR in i.i.d. Rician and Nakagami-*m* fadings, respectively. Note that the switching rate in Rician fading depends only on K, while in Nakagami-*m* fading it only depends on m, as proved in the previous section. In addition, when $K = 0$ or $m = 1$, Rician or Nakagami-*m* fading reduces

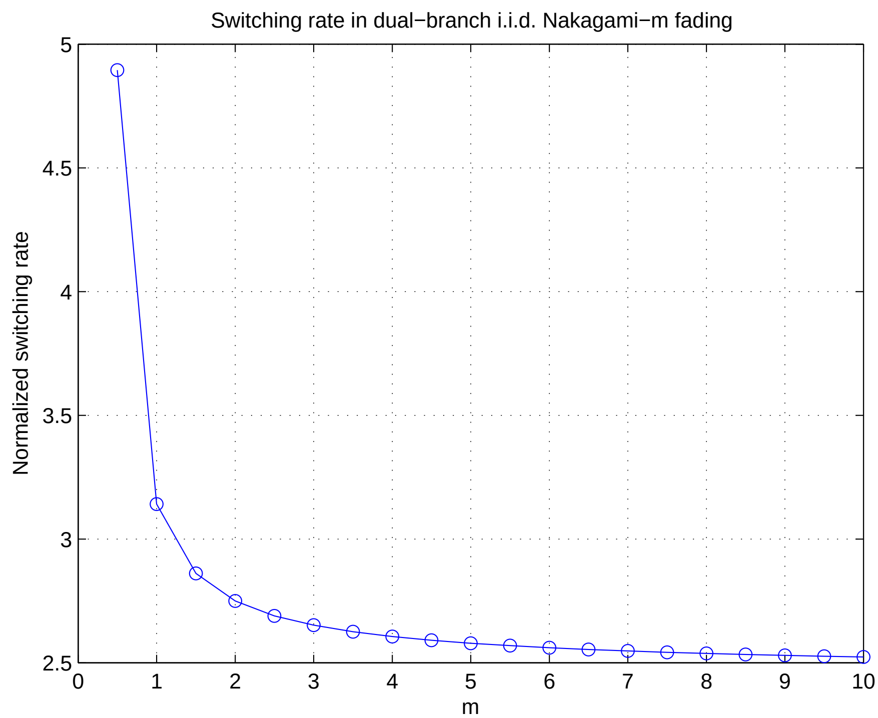

Figure 5.4. The normalized switching rates vs m of opportunistic relaying in i.i.d. Nakagami-*m* fading channels.

to Rayleigh fading, and the switching rates have the same value (π), in agreement with the results presented in [11]. One could then compare the switching rate in Rayleigh fading to that in Rician and Nakagami fading. Finally, as expected, as K or m becomes larger, the switching rates become smaller with diminishing increases. This is because as K and m become larger, the severity of the fading process becomes less significant, and the channel amplitudes fluctuate less.

5.3 The Contrasting Behaviors in Rician and Nakagami-m Fading of Switching Rate of Switch-and-Examine Relaying

Comparing the results in Fig. 5.1 and with the results in Fig. 5.2, one can observe that the switching rates of switch-and-examine relaying in Rician fading and Nakagami-*m* fading behave quite differently. The shapes of the switching rate curves in Rician fading shift toward higher threshold. This is due to the fact that even though Rician random variables can sometimes approximate Nakagami-*m* random variables [14], the PDF and CDF of the minimum of two Rician random variables is very different from that of the Nakagami-*m* random variables. The underlying reason is that the tails of the PDFs of these random variables are not similar. See (4.7) which shows explicitly the dependence of the switching rate on the PDF of R_i. Further insight into the issue of why the Nakagami-*m* distribution is not a good approximation for the Rician distribution is obtained graphically from Fig. 5.5 and Fig. 5.6. The PDFs of the minimum of two Rician random variables and two Nakagami-*m* random variables for different values of ν and m are plotted in Fig. 5.5. Note that $\sigma = 1$ and $\Omega = 2$ for all PDFs. One can see that gross differences exist between the two distributions. To examine carefully the behaviors of the tails of the two distributions, Fig. 5.6 shows the PDFs on a logarithmic scale. One can see that the tails of the PDF in the Rician cases have the same slopes regardless of the values of ν_i. In contrast, the slopes of the tails of the PDFs in the Nakagami-*m* cases vary with the values of m_i. This dramatically different behavior of the Rician and Nakagami-*m* tails has been noted before in the context of receiver diversity

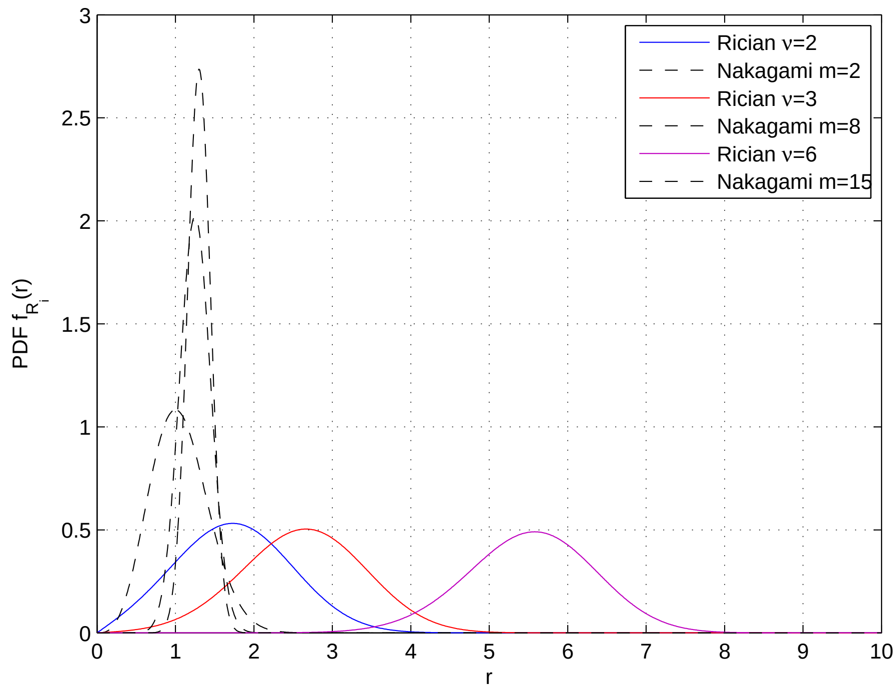

Figure 5.5. The PDFs of the minimum of two Rician random variables and two Nakagami-*m* random variables for different values of ν and m with $\sigma = 1$ and $\Omega = 2$.

systems.

5.4 Bit Error Rate and Switching Rate in Switch-and-Examine Relaying

The choice of switching threshold (R_{th}) will affect both the switching rate and the BER of the system. Since a complete treatment of the bit error rate of switch-and-examine relaying in Rician and Nakagami-*m* fading is beyond the scope of this thesis, we use simulation to illustrate the interrelationship between switching rate, BER and R_{th}. Efficient procedures for generating Nakagami-*m* and Rician random variates are found in [29] and [30]. In the simulation[2], we assume the unfaded SNR to be 0 db for Rician fading and 5 db for Nakagami-*m* fading. Binary phase-shift

[2]In this simulation, we assume channel conditions are independent in time. Future research could investigate scenarios where channel conditions are correlated in time

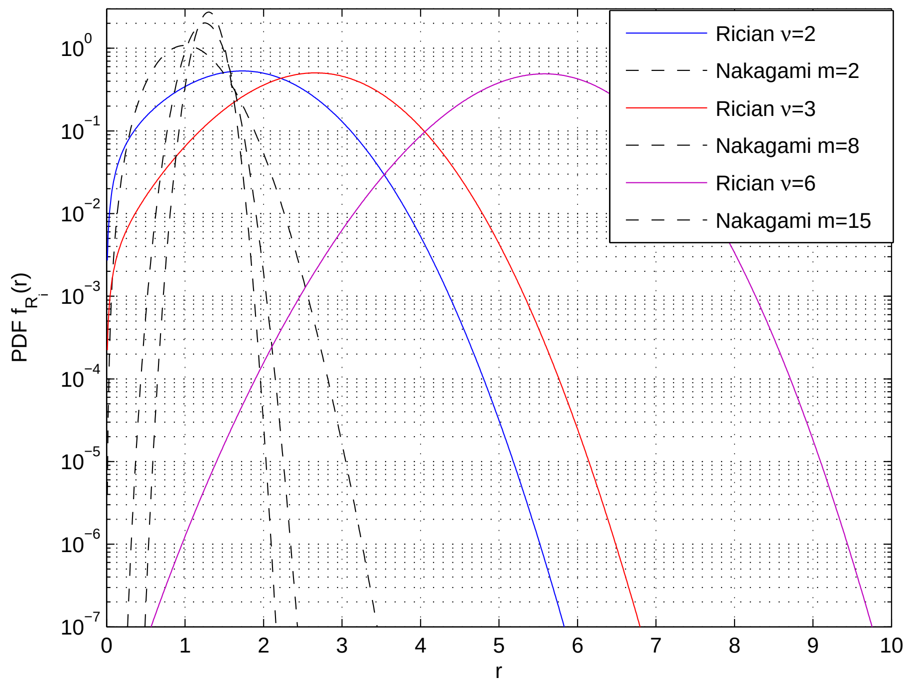

Figure 5.6. The PDFs of the minimum of two Rician random variables and two Nakagami-*m* random variables on a logarithmic scale for different values of ν and m with $\sigma = 1$ and $\Omega = 2$.

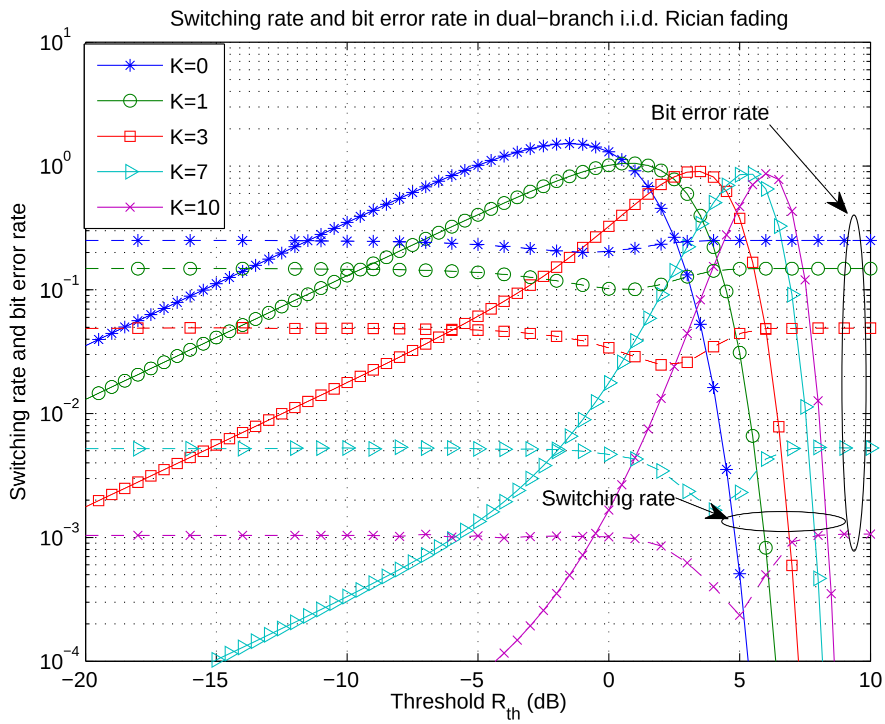

Figure 5.7. The switching rates (solid line) and bit error rate (dashed line) of switch-and-examine relaying in i.i.d. Rician fading channels for different values of K with $\sigma = 1$.

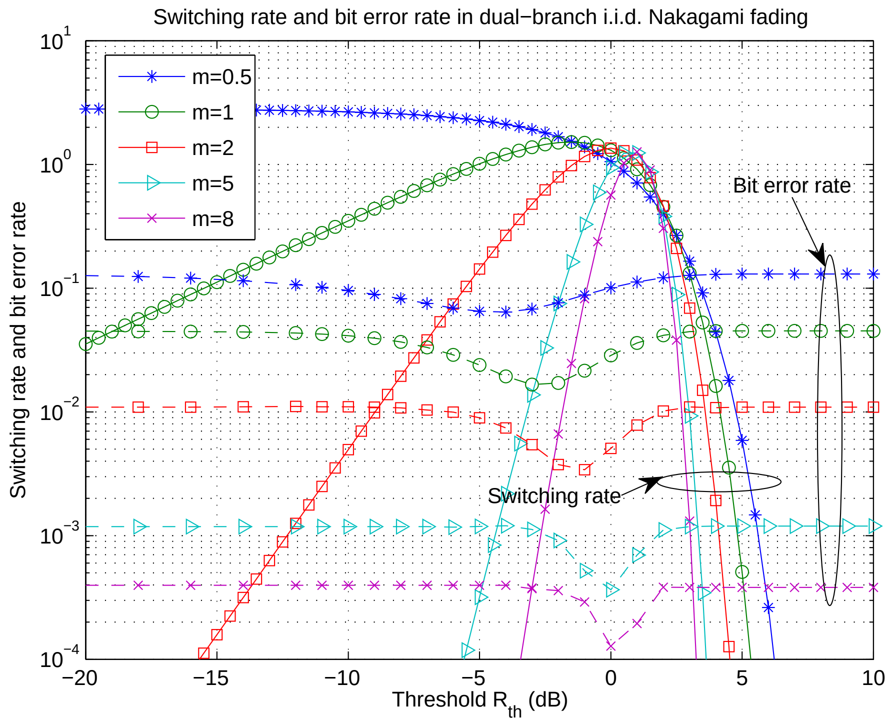

Figure 5.8. The switching rates (solid line) and bit error rate (dashed line) of switch-and-examine relaying in i.i.d. Nakagami-*m* fading channels for different values of m with $\Omega = 2$.

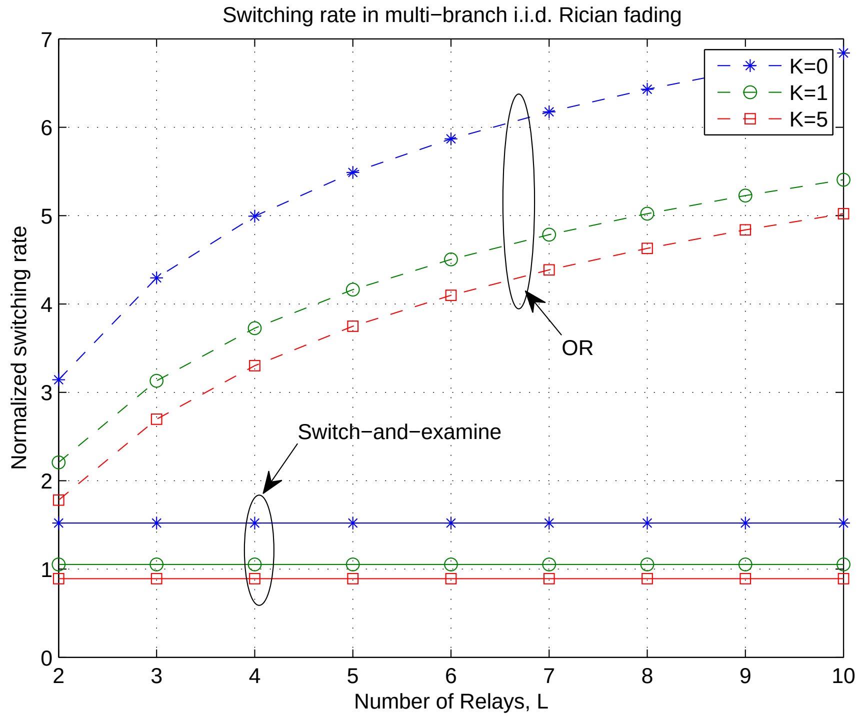

Figure 5.9. The normalized switching rates of i.i.d. multi-branch opportunistic relaying and switch-and-examine relaying in Rician fading channels for different values of K.

keying (BPSK) is used for modulation. Also no direct signal path between source and destination is available. We further assume that the system has no receiver outage, perfect channel estimation and perfect synchronization. For simplicity, only the BER of DF is plotted. Fig. 5.7 and Fig. 5.8 show the switching rate and BER vs R_{th} in Rician fading and Nakagami-*m* fading for different values of K and m. Examination reveals that for all K and m, the value of R_{th} that yields small BER simultaneously leads to relatively high switching rate. However, the value of R_{th} that minimizes the BER does not yield the maximum switching rate. Depending on the system's requirements on BER and switching rate, one can use the results and methods of this thesis to choose R_{th} to meet the design objectives.

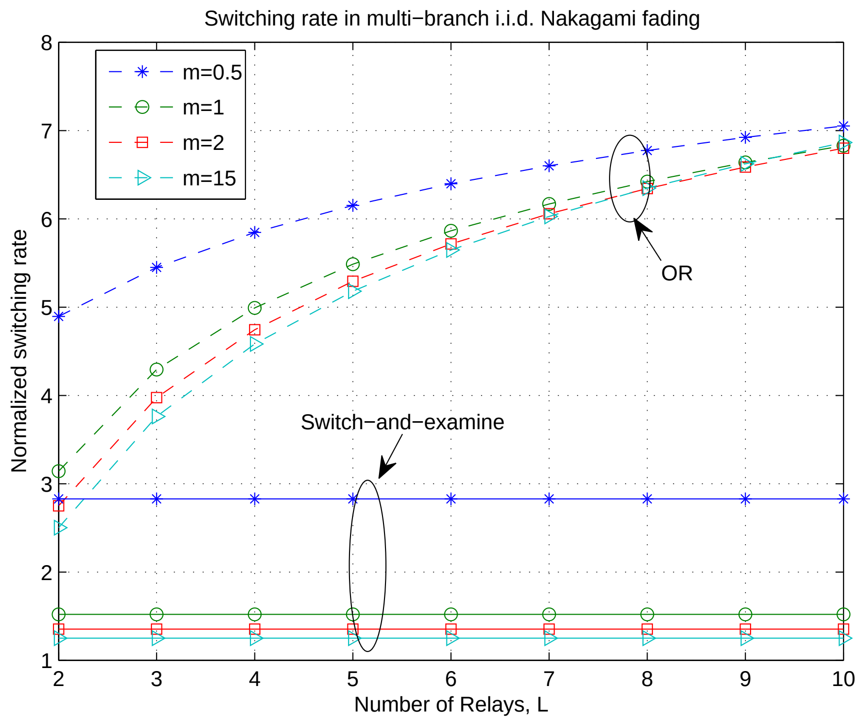

Figure 5.10. The normalized switching rates of i.i.d. multi-branch opportunistic relaying and switch-and-examine relaying in Nakagami-*m* fading channels for different values of m.

5.5 Switching Rate in Multi-Branch Systems

Next we investigate switching rate in multi-branch systems. Fig. 5.9 shows the normalized switching rates of multi-branch opportunistic relaying and the maximum switching rate of switch-and-examine relaying in i.i.d. Rician fading with $\sigma = 2$ for different values of K. Fig. 5.10 shows similar results for i.i.d. Nakagami fading with $\Omega = 2$ and $m = 3$. In both cases, the switching rate of OR increases nonlinearly with the number of relays while that of switch-and-stay relaying is independent of the number of relays. In this regard, as the number of relays becomes larger, switch-and-stay relaying becomes more and more attractive for practical implementations where the switching rate is a concern.

5.6 Switching Rate in Unbalanced Systems

We now consider switching rates in dual-branch i.n.i.d. fadings. For simplicity, we assume every link has the same maximum Doppler shift, f_m. Furthermore, we assume that R_{Si} and R_{iD} have the same distributions while R_{S1} and R_{S2} have different distributions. Specifically, for Rician fading, let $\sigma_{S1} = \sigma_{1D} = 1$, $\sigma_{S2} = \sigma_{2D} = 2$, $K_{S1} = K_{1D} = K$ and $K_{S2} = K_{2D} = 1.5K$. For Nakagami-*m* fading, let $\Omega_{S1} = \Omega_{1D} = 2$, $\Omega_{S2} = \Omega_{2D} = 6$, $m_{S1} = m_{1D} = m$ and $m_{S2} = m_{2D} = 2m$. The switching rates in Rician and Nakagami-*m* fading with these parameters are plotted in Fig. 5.11 and Fig. 5.12 for different values of K and m. As seen in the figure, the switching rate of opportunistic relaying is comparable to that of switch-and-examine relaying. The reason is that if the channels are highly unbalanced, both systems will likely dwell on the superior node. Similar behavior has been noted in [8] for switching rates in conventional selection combining and switch-and-stay combining. It is also worth noticing that as K or m becomes larger, the maximum switching rates in unbalanced scenarios reduce faster compared to those in i.i.d. cases.

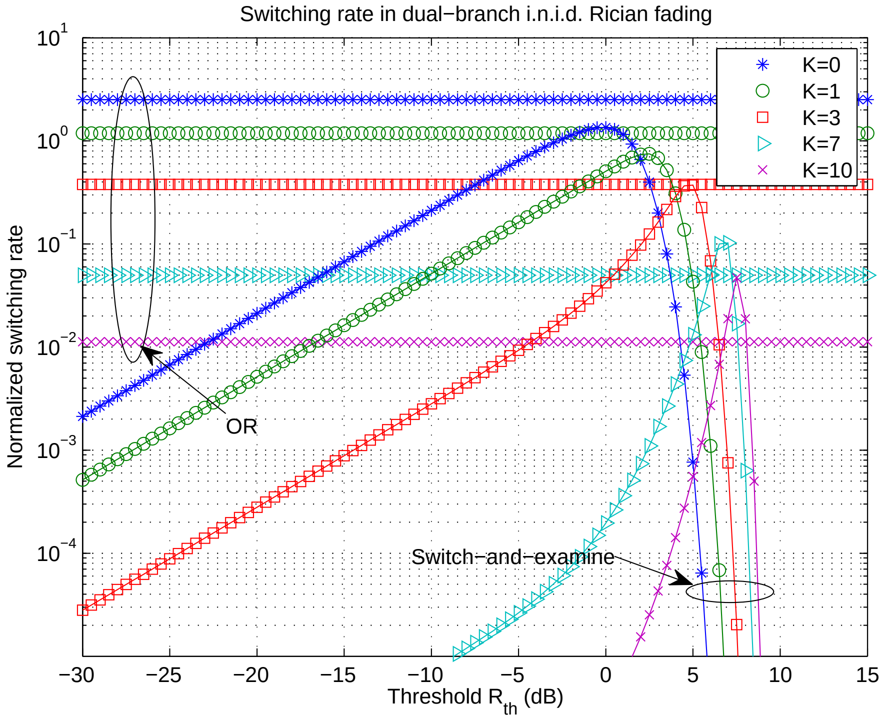

Figure 5.11. The normalized switching rates of opportunistic relaying and switch-and-examine relaying in unbalanced Rician fading channels for different values of K. The details of the specific configuration are given in Section 5.

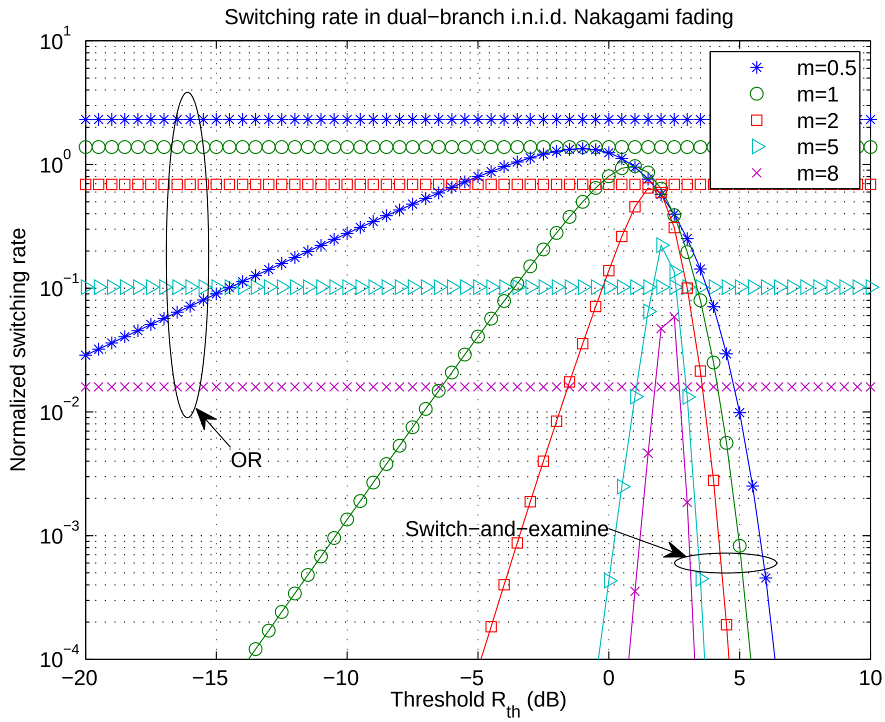

Figure 5.12. The normalized switching rates of opportunistic relaying and switch-and-examine relaying in unbalanced Nakagami-*m* fading channels for different values of m. The details of the specific configuration are given in Section 5.

Chapter 6

Conclusion and Suggestions for Future Work

In this chapter, we present the conclusion and provide some future research directions.

6.1 Conclusions

In this thesis, we investigated the switching rates, that is, how frequently the system switches from one relay to another, of opportunistic relaying and switch-and-examine relaying in Rician and Nakagami-*m* fading.

- We derived the switching rate for opportunistic relaying in Chapter 3. Specifically, under Rician fading, the switching rate for opportunistic relaying was expressed as a single integral, which can easily be evaluated numerically. In addition, we derived closed-form solutions for the switching rate under Nakagami-*m* fading for both dual-branch and multi-branch relaying. Such solutions can further facilitate the evaluation of switching rate.

- In Chapter 4, building on the previous results, we derived the switching rate for switch-and-examine relaying systems. Exact closed-form solutions are available for Rician and Nakagami-*m* fading. We find that the switching rate of multi-branch switch-and-examine relaying systems does not depend on the number of relays, L. This fact can be used to bring about significant advantage compared to opportunistic relaying in multi-branch settings.

- We presented numerical results in Chapter 5. The results for opportunistic relaying and switch-and-examine relaying were compared. The tradeoff between switching rate and bit error rate was also explored. We also demonstrated the effect of different parameters on the switching rates.

6.2 Suggestions for Future Research Directions

Based on this thesis, some possible future research directions are given below.

- In the system model of this thesis, only one relay is selected at a given time. One can consider systems where more than one relay is selected at a given time, for example relay systems similar to those in [7].

- One could derive the switching rates for opportunistic relaying and switch-and-examine relaying under other fading models by applying the methodology used in this thesis. For example, one could consider fading models in non-homogeneous scattering environment, such as κ-μ fading and η-μ fading [31].

- In this thesis, it is assumed that the fading process and its time-derivative process are independent. It could be interesting to explore the switching rate in the case where they are correlated.

- In this thesis, the tradeoff between switching rate and bit error rate is demonstrated in the numerical results. For practical implementation, one may need a better understanding of this tradeoff. Thus, it will be interesting to investigate quantitatively how the the switching threshold impacts switching rate, bit error rate and outage probability and how such impact translates to practical implementation.

- One could investigate more thoroughly the performance of switch-and-examine relaying systems in that its simplicity and low switching rate make it a suitable candidate for practical implementation.

- It would be highly desirable to propose and analyze some hybrid protocols that take advantage the low bit error rate of opportunistic relaying and low switching rate of switch-and-examine relaying. Such protocols, if carefully designed and calibrated, could be used widely in the telecommunication industry.

- When evaluating conventional diversity systems and cooperative communication systems, researchers usually focus on bit error rate and outage probability performance without considering the detrimental effect of switching rate in such systems. In order to address a host of practical implementation issues, researchers must consider switching rate. It would be interesting to revisit the overall performance of selection combining and opportunistic relaying in realistic settings while considering switching rate.

Appendix A

Dual-Branch System

A.1 Derivation of $f_Z(0)$ for Integer m

In this appendix, we derive the closed-form solution for $f_Z(0)$ in Nakagami-*m* fading with integer m. For notational simplicity, we denote $\alpha = \frac{m}{\Omega}$ throughout this appendix. If m is an integer, by using [16, eq.(8.352.2)] one has

$$\Gamma(m, r) = \Gamma(m) \exp(-r) \sum_{k=0}^{m-1} \frac{r^k}{k!} \tag{A.1}$$

and we can write (3.9) as

$$f_{R_i}(r) = \frac{4\alpha^m}{\Gamma(m)} \exp(-2\alpha r^2) \sum_{k=0}^{m-1} \alpha^k \frac{r^{2(k+m)-1}}{k!}. \tag{A.2}$$

Therefore, (3.14) can be written as

$$\begin{aligned} f_Z(0) &= \frac{16\alpha^{2m}}{\Gamma^2(m)} \int_0^\infty \exp(-4\alpha r^2) \sum_{i=0}^{m-1} \alpha^i \frac{r^{2(i+m)-1}}{i!} \sum_{j=0}^{m-1} \alpha^j \frac{r^{2(j+m)-1}}{j!} \, dr \qquad &\text{(A.3)} \\ &= \frac{16\alpha^{2m}}{\Gamma^2(m)} \sum_{i=0}^{m-1} \sum_{j=0}^{m-1} \frac{\alpha^{i+j}}{i!j!} \int_0^\infty \exp(-4\alpha r^2) r^{2(i+j+2m)-2} \, dr. \qquad &\text{(A.4)} \end{aligned}$$

The integral in (A.4) is simply a combination of exponential functions and power functions, its closed-form solution is readily available in [16, eq. (3.381.4)]. After applying [16, eq. (3.381.4)] and some manipulation, we obtain the closed-form solution for $f_Z(0)$

$$f_Z(0) = \frac{\sqrt{\frac{m}{\Omega}}}{4^{2m-2}\Gamma^2(m)} \sum_{i=0}^{m-1} \sum_{j=0}^{m-1} \frac{\Gamma(i+j+2m-0.5)}{i!j!4^{i+j}}. \tag{A.5}$$

One can obtain $f_Z(0)$ in i.n.i.d. cases by giving appropriate indices to α, m and Ω and following the procedures above.

A.2 Derivation of $f_Z(0)$ for Non-Integer m

In this appendix, we derive the closed-form solution for $f_Z(0)$ in Nakagami-*m* fading with non-integer m. By using $\Gamma(a,b) = \Gamma(a) - \gamma(a,b)$ and the substitution $x = r^2$, $f_Z(0)$ can be expressed as

$$f_Z(0) = \frac{16\alpha^{2m}}{\Gamma^4(m)} \int_0^\infty x^{2m-\frac{3}{2}} \exp\left(-2\alpha x\right) \left[\Gamma(m) - \gamma\left(m, \alpha x\right)\right]^2 \, dx. \tag{A.6}$$

Letting $C = \frac{16\alpha^{2m}}{\Gamma^4(m)}$ and expanding $\left[\Gamma(m) - \gamma\left(m, \alpha x\right)\right]^2$, we have

$$\begin{aligned} f_Z(0) =& C\Gamma^2(m) \int_0^\infty x^{2m-\frac{3}{2}} \exp\left(-2\alpha x\right) \, dx \\ & - 2C\Gamma(m) \int_0^\infty x^{2m-\frac{3}{2}} \exp\left(-2\alpha x\right) \gamma(m, \alpha x) \, dx \\ & + C \int_0^\infty x^{2m-\frac{3}{2}} \exp\left(-2\alpha x\right) \gamma^2(m, \alpha x) \, dx. \end{aligned} \tag{A.7}$$

The first two integrals in (A.7) can be evaluated using [16, eq. (3.381.4)] and [16, eq. (6.455.2)], while the last integral can be evaluated with the help of [32, eq. (10)]. Now we have the closed-form for $f_Z(0)$,

$$\begin{aligned} f_Z(0) = & C \frac{\alpha^{2m}\Gamma(4m-\frac{1}{2})}{m^2(4\alpha)^{4m-\frac{1}{2}}} F_2(4m-\frac{1}{2}, 1, 1, 1+m, 1+m; \frac{1}{4}, \frac{1}{4}) \\ & + C\Gamma^2(m) \frac{\Gamma(2m-\frac{1}{2})}{(2\alpha)^{2m-\frac{1}{2}}} - 2C\Gamma(m) \frac{\alpha^m \Gamma(3m-\frac{1}{2})}{m(3\alpha)^{3m-\frac{1}{2}}} {}_2F_1(1, 3m-\frac{1}{2}; m+1; \frac{1}{3}) \end{aligned} \tag{A.8}$$

where $F_2(\alpha, \beta, \beta', \gamma, \gamma'; x, y)$ is the hypergeometric function of two variables defined in [16, eq. (9.180.2)] as

$$F_2(\alpha, \beta, \beta', \gamma, \gamma'; x, y) = \sum_{m=0}^\infty \sum_{n=0}^\infty \frac{(\alpha)_{m+n}(\beta)_m(\beta')_n}{(\gamma)_m(\gamma')_n m! n!} x^m y^n \tag{A.9}$$

and the notation $(a)_n = \Gamma(a+n)/\Gamma(a)$ denotes the Pochhammer symbol defined at [16, xliii]. It should be pointed out that despite its seemingly simplicity, this closed-form solution may not be computationally efficient since (A.9) involves two infinite summations and is not implemented in popular mathematics packages such as MATLAB and Mathematica. In addition, one can obtain $f_Z(0)$ in i.n.i.d. cases by giving appropriate indices to α, m, Ω and C and following the procedures above.

Appendix B

Multi-Branch System

B.1 Derivation of the Integral in (3.57) for Integer m

In this appendix, we derive the closed-form solution for the integral in (3.57) (denoted as I) for multi-branch systems experiencing Nakagami-*m* fading with integer m. If we use the substitution $x = r^2$ and (A.1), I can be written as

$$I = \frac{1}{2}\int_0^{\infty} x^{2m-\frac{3}{2}} \exp\left(-4mx\right) \left(\sum_{l=0}^{m-1} \frac{m^l}{l!}x^l\right)^2 \cdot \left[1 - \exp\left(-2mx\right)\left(\sum_{l=0}^{m-1}\frac{m^l}{l!}x^l\right)^2\right]^{L-2} dx. \tag{B.1}$$

By employing binomial and multinomial theorems, I can be converted into the summation of a series of simple integrals as follows,

$$I = \frac{1}{2}\sum_{i=0}^{L-2}\binom{L-2}{i}(-1)^i \int_0^{\infty} x^{2m-\frac{3}{2}} \exp\left[-(4+2i)mx\right]\left[\sum_{l=0}^{m-1}\frac{m^l}{l!}x^l\right]^{2i+2} dx \tag{B.2}$$

$$= \frac{1}{2}\sum_{i=0}^{L-2}\binom{L-2}{i}(-1)^i \int_0^{\infty} x^{2m-\frac{3}{2}} \exp\left[-(4+2i)mx\right] \cdot \sum_{\substack{k_0,k_1,\ldots,k_{m-1}\\ k_0+\ldots+k_{m-1}=2i+2}} \binom{2i+2}{k_0,k_1,\ldots,k_{m-1}} \prod_{l=0}^{m-1}\left[\frac{m^l}{l!}x^l\right]^{k_l} dx \tag{B.3}$$

$$= \frac{1}{2}\sum_{i=0}^{L-2}\binom{L-2}{i}(-1)^i \sum_{\substack{k_0,k_1,\ldots,k_{m-1}\\ k_0+\ldots+k_{m-1}=2i+2}} \binom{2i+2}{k_0,k_1,\ldots,k_{m-1}} \prod_{l=0}^{m-1}\left(\frac{m^l}{l!}\right)^{k_l}$$

$$\cdot \int_0^\infty \exp\left[-(4+2i)mx\right] x^{\mu-1}\, dx \tag{B.4a}$$

where we use

$$\binom{n}{k_0, k_1, ..., k_{m-1}} = \frac{n!}{k_0! k_1! \cdots k_{m-1}!} \tag{B.4b}$$

$$\mu = \sum_{i=0}^{m-1} i k_i + 2m - 0.5. \tag{B.4c}$$

In (B.2), we use the well known binomial theorem, $(1-a)^n = \sum_{i=0}^{n} \binom{n}{i} (-1)^i a^i$. In (B.3), we use the multinomial theorem, namely

$$(x_0 + x_1 + ... + x_{m-1})^n = \sum_{\substack{k_0, k_1, ..., k_{m-1} \\ k_0 + ... + k_{m-1} = n}} \binom{n}{k_0, k_1, ..., k_{m-1}} \prod_{l=0}^{m-1} x_l^{k_l}. \tag{B.5}$$

In (B.4a), we simply take the integral inside the summation. Now the integral in (B.4a) is simply a combination of exponentials and powers and can be solved by using [16, eq. (3.381.4)]. After some manipulation, we obtain the closed-form solution for I.

$$I = \frac{m^{0.5-2m}}{2} \sum_{i=0}^{L-2} \binom{L-2}{i} (-1)^i \sum_{\substack{k_0, k_1, ..., k_{m-1} \\ k_0 + ... + k_{m-1} = 2i+2}} \frac{\Gamma(\mu)}{(4+2i)^\mu}$$

$$\cdot \binom{2i+2}{k_0, k_1, ..., k_{m-1}} \prod_{l=0}^{m-1} \left(\frac{1}{l!}\right)^{k_l}. \tag{B.6}$$

Note that if $L = 2$, the switching rate will reduce to that of dual-branch cases. The proof is the following. Since $L = 2$, (B.6) reduces to,

$$I = \frac{m^{0.5-2m}}{2} \sum_{\substack{k_0, k_1, ..., k_{m-1} \\ k_0 + ... + k_{m-1} = 2}} \frac{\Gamma(\mu)}{4^\mu} \binom{2}{k_0, k_1, ..., k_{m-1}} \prod_{l=0}^{m-1} \left(\frac{1}{l!}\right)^{k_l}. \tag{B.7}$$

Since k_i can only be integer, there are two different scenarios, either $k_i = 2, (0 \leq i \leq m-1)$ or $k_i = 1, k_j = 1, (i \neq j, 0 \leq i \leq m-1, 0 \leq j \leq m-1)$. Therefore, I becomes

$$I = \frac{m^{0.5-2m}}{4^{2m}} \left[\sum_{i=0}^{m-1} \frac{\Gamma(2i + 2m - 0.5)}{(i!)^2 4^{2i}} + \sum_{i=0}^{m-1} \sum_{j=0, j\neq i}^{m-1} \frac{\Gamma(i + j + 2m - 0.5)}{i! j! 4^{i+j}} \right] \tag{B.8}$$

$$= \frac{m^{0.5-2m}}{4^{2m}} \sum_{i=0}^{m-1} \sum_{j=0}^{m-1} \frac{\Gamma(i + j + 2m - 0.5)}{i! j! 4^{i+j}}. \tag{B.9}$$

When $L = 2$, the constant before the integral in (3.57) is $\frac{32\sqrt{\pi} f_m}{\Gamma^2(m)} m^{2m-\frac{1}{2}}$. The switching rate thus becomes identical to (3.43)

$$SR_{OR} = \frac{2 f_m \sqrt{\pi}}{4^{2m-2}\Gamma^2(m)} \sum_{i=0}^{m-1} \sum_{j=0}^{m-1} \frac{\Gamma(i+j+2m-0.5)}{i!j!4^{i+j}}. \tag{B.10}$$

B.2 Derivation of the Integral in (3.57) for Non-Integer m

If m is not an integer, the substitution $x = r^2$ and $\Gamma(a,b) = \Gamma(a) - \gamma(a,b)$ are made. After some manipulation, I becomes

$$\begin{aligned} I =& \frac{1}{2\Gamma^{2L-2}(m)} \int_0^\infty x^{2m-\frac{3}{2}} \exp\left(-2mx\right) \left[\Gamma(m) - \gamma(m,mx)\right]^2 \\ & \cdot \gamma^{L-2}(m,mx) \left[2\Gamma(m) - \gamma(m,mx)\right]^{L-2} \, dx. \end{aligned} \tag{B.11}$$

Let $P = \frac{1}{2\Gamma^{2L-2}(m)}$ and $f(x) = x^{2m-\frac{3}{2}} \exp\left(-2mx\right)$. Using the binomial theorem to expand $\left[2\Gamma(m) - \gamma(m,mx)\right]^{L-2}$, the integral becomes

$$I =P \int_0^\infty f(x)[\Gamma^2(m) - 2\Gamma(m)\gamma(m,mx) + \gamma^2(m,mx)] \sum_{i=0}^{L-2} c_i \gamma^{L-2+i}(m,mx) \, dx \tag{B.12a}$$

where

$$c_i = \binom{L-2}{i} \left[2\Gamma(m)\right]^{L-2-i} (-1)^i. \tag{B.12b}$$

Eq. (B.12a) can be reorganized as

$$\begin{aligned} I = & P\Gamma^2(m) \sum_{i=0}^{L-2} c_i \int_0^\infty f(x)\gamma^{L-2+i}(m,mx) \, dx \\ & - 2P\Gamma(m) \sum_{i=0}^{L-2} c_i \int_0^\infty f(x)\gamma^{L-1+i}(m,mx) \, dx \\ & + P \sum_{i=0}^{L-2} c_i \int_0^\infty f(x)\gamma^{L+i}(m,mx) \, dx. \end{aligned} \tag{B.13}$$

With the help of [32, eq. (10)], we define a new function $g(m,s)$ as

$$g(m,s) = \int_0^\infty f(x)\gamma^s(m,mx)\,dx = \frac{(m)^{ms}\Gamma(2m+sm-\frac{1}{2})}{m^s[2m+sm]^{2m+sm-\frac{1}{2}}}$$
$$\cdot F_A\left(2m+sm-\frac{1}{2};\underbrace{1,\ldots,1}_{s\text{ terms}};\underbrace{1+m,\ldots,1+m}_{s\text{ terms}};\underbrace{\frac{1}{2+s},\ldots,\frac{1}{2+s}}_{s\text{ terms}}\right) \quad \text{(B.14)}$$

where $F_A(\cdot;\cdot;\cdot;\cdot)$ is Lauricella's hypergeometric function of several variables and is defined as [16, eq. (9.19)]

$$F_A(\alpha;\beta_1,\ldots,\beta_s;\gamma_1,\ldots,\gamma_s;z_1,\ldots,z_s;)$$
$$= \sum_{m_1=0}^{\infty}\cdots\sum_{m_s=0}^{\infty}\frac{(\alpha)_{m_1+\cdots+m_s}(\beta_1)_{m_1}\ldots(\beta_s)_{m_s}}{(\gamma_1)_{m_1}\ldots(\gamma_s)_{m_s}m_1!\ldots m_s!}z_1^{m_1}\ldots z_s^{m_s}. \quad \text{(B.15)}$$

Therefore, by substituting (B.14) into (B.13), one can obtain a closed-form expression for I as

$$I = P\Gamma^2(m)\sum_{i=0}^{L-2}c_i g(m,L-2+i) - 2P\Gamma(m)\sum_{i=0}^{L-2}c_i g(m,L-1+i)$$
$$+ P\sum_{i=0}^{L-2}c_i g(m,L+i) \quad \text{(B.16)}$$

with c_i and $g(m,s)$ defined in (B.12b) and (B.14), respectively. Note that the computational complexity of (B.16) may well exceed that of the single integral in (3.57) since it involves multiple infinite summations, especially when L is large. In addition, the Lauricella's hypergeometric function is not implemented in popular mathematics packages such as MATLAB and Mathematica. When $L = 2$, the expression for the switching rate will reduce to the expression for the dual-branch case in (A.8).

References

[1] J. N. Laneman, D. N. C. Tse, and G. W. Wornell, “Cooperative diversity in wireless networks: Efficient protocols and outage behavior,” *IEEE Trans. Inf. Theory*, vol. 50, no. 12, pp. 3062–3080, Dec. 2004.

[2] J. N. Laneman and G. W. Wornell, “Distributed space-time coded protocols for exploiting cooperative diversity in wireless networks,” *IEEE Trans. Inf. Theory*, vol. 49, no. 10, pp. 2415–2525, Oct. 2003.

[3] A. Bletsas, A. Khisti, D. P. Reed, and A. Lippman, “A simple cooperative diversity method based on network path selection,” *IEEE J. Sel. Areas Commun.*, vol. 24, no. 3, pp. 659–672, Mar. 2006.

[4] Y. Jing and H. Jafarkhani, “Single and multiple relay selection schemes and their achievable diversity orders,” *IEEE Trans. Wireless Commun.*, vol. 8, no. 3, pp. 1414–1423, Mar. 2009.

[5] A. A. Abu-Dayya and N. C. Beaulieu, “Analysis of switched diversity systems on generalized-fading channels,” *IEEE Trans. Commun.*, vol. 42, no. 11, pp. 2959–2966, Nov. 1994.

[6] D. S. Michalopoulos and G. K. Karagiannidis, “Two-relay distributed switch and stay combining,” *IEEE Trans. Commun.*, vol. 56, no. 11, pp. 1790–1794, Nov. 2008.

[7] J. K. Cavers and P. Ho, “Switching rate and dwell time in m-of-n selection diversity,” *IEEE Trans. Wireless Commun.*, vol. 6, no. 4, pp. 1218–1223, Apr. 2007.

[8] N. C. Beaulieu, “Switching rates of selection diversity and switch-and-stay diversity,” in *Proc. IEEE Int. Conf. Commun. (ICC)*, Beijing, China, May 2008, pp. 4671–4677.

[9] N. C. Beaulieu, “Switching rates of dual selection diversity and dual switch-and-stay diversity,” *IEEE Trans. Commun.*, vol. 56, pp. 1409–1413, Sep. 2008.

[10] N. C. Beaulieu and A. A. Abu-Dayya, “The evaluation of error probabilities for low-frequency attenuation channels,” *IEEE Trans. Commun.*, vol. 42, no. 9, pp. 2676–2683, Sep. 1994.

[11] D. S. Michalopoulos, A. S. Lioumpas, G. K. Karagiannidis, and R. Schober, “Selective cooperative relaying over time-varying channels,” *IEEE Trans. Commun.*, vol. 48, no. 8, pp. 2402–2412, Aug. 2010.

[12] H.-C. Yang and M.-S. Alouini, “Markov chains and performance comparison of switched diversity systems,” *IEEE Trans. Commun.*, vol. 52, no. 7, pp. 1113–1125, Jul. 2004.

[13] A. Goldsmith, *Wireless Communications*. Cambridge University Press, 2005.

[14] G. L. Stüber, *Principles of Mobile Communication*, 2nd ed. Norwell, MA: Kluwer Academic Publishers, 2002.

[15] J. G. Proakis, *Digital Communications*, 5th ed. New York: McGraw-Hill, Inc., 2007.

[16] I. S. Gradshteyn and I. M. Ryzhik, *Table of Integrals, Series, and Products*, 6th ed. New York: Academic, 2000.

[17] M. K. Simon, *Probability Distributions Involving Gaussian Random Variables: A Handbook for Engineers and Scientists*. Boston, MA: Kluwer, 2002.

[18] N. C. Beaulieu and A. M. Rabiei, “Linear diversity combining on Nakagami-0.5 fading channels,” *IEEE Trans. Commun.*, vol. 59, no. 10, pp. 2742–2752, Oct. 2011.

[19] A. Behnad, N. C. Beaulieu, and B. Maham, “Multi-hop amplify-and-forward relaying on Nakagami-0.5 fading channels,” *IEEE Wireless Communications Letters*, to appear 2012.

[20] M. O. Hasna and M. S. Alouini, “Harmonic mean and end-to-end performance of transmission systems with relays,” *IEEE Trans. Commun.*, vol. 52, no. 1, pp. 130–135, Jan. 2004.

[21] C. S. Patel and G. L. Stüber, “Channel estimation for amplify and forward relay based cooperation diversity systems,” *IEEE Trans. Wireless Commun.*, vol. 6, no. 6, pp. 2348–2356, Jun. 2007.

[22] F. Gao, T. Cui, and A. Nallanathan, “On channel estimation and optimal training design for amplify and forward relay networks,” *IEEE Trans. Wireless Commun.*, vol. 7, no. 5, pp. 1907–1916, May 2008.

[23] C. Xiao and N. C. Beaulieu, “Node switching rates of opportunistic relaying in Rician and Nakagami-*m* fading,” in *Proc. IEEE GLOBECOM Conf.*, Houston, Texas, USA, Dec. 5-9, 2011.

[24] C. Xiao and N. C. Beaulieu, “Node switching rates of opportunistic relaying and switch-and-examine relaying in Rician and Nakagami-*m* fading,” *IEEE Trans. Commun.*, vol. 60, no. 2, pp. 488–498, Feb. 2012.

[25] A. Papoulis and S. U. Pillai, *Probability, Random Variables and Stochastic Processes*, 4th ed. New York: McGraw-Hill, Inc., 2002.

[26] M. Schwartz, W. R. Bennett, and S. Stein, *Communication Systems and Techniques*, 2nd ed. New York: McGraw-Hill, Inc., 1966.

[27] M. D. Yacoub, J. E. V. Bautista, and L. G. de Rezende Guedes, “On higher order statistics of the Nakagami-*m* distribution,” *IEEE Trans. Veh. Technol.*, vol. 48, pp. 790–794, May 1999.

[28] C. Xiao and N. C. Beaulieu, "Node switching rates of switch-and-examine relaying in Rician and Nakagami-*m* fading," in *Proc. European Wireless 2011*, Vienna, Austria, Apr. 27-29, 2011, pp. 569–574.

[29] N. C. Beaulieu and C. Cheng, "Efficient Nakagami-*m* fading channel simulation," *IEEE Trans. Veh. Technol.*, vol. 54, no. 3, pp. 413–424, Mar. 2005.

[30] D. J. Young and N. C. Beaulieu, "The generation of correlated Rayleigh random variates by inverse discrete Fourier transform," *IEEE Trans. Commun.*, vol. 48, no. 7, pp. 1114–1127, Jul. 2000.

[31] M. D. Yacoub, "The κ-μ distribution and the η-μ distribution," *IEEE Antennas Propag. Mag.*, vol. 49, no. 1, pp. 68–81, Feb. 2007.

[32] J. M. Romero-Jerez and A. J. Goldsmith, "Performance of multichannel reception with transmit antenna selection in arbitrarily distributed Nakagami fading channels," *IEEE Trans. Wireless Commun.*, vol. 8, no. 4, pp. 2006–2013, Apr. 2009.